PREPARATION OF SILICA COATED COBALT FERRITE MAGNETIC NANOPARTICLES FOR THE PURIFICATION OF HISTIDINE-TAGGED PROTEINS

A THESIS SUBMITTED TO
THE GRADUATE SCHOOL OF NATURAL AND APPLIED SCIENCES
OF
MIDDLE EAST TECHNICAL UNIVERSITY

BY

GÜLFEM AYGAR

IN PARTIAL FULFILLMENT OF THE REQUIREMENTS
FOR
THE DEGREE OF MASTER OF SCIENCE
IN
MICRO AND NANOTECHNOLOGY

OCTOBER 2011

Approval of the Thesis:

PREPARATION OF SILICA COATED COBALT FERRITE MAGNETIC NANOPARTICLES FOR THE PURIFICATION OF HISTIDINE-TAGGED PROTEINS

submitted by **GÜLFEM AYGAR** in partial fulfillment of the requirements for the degree of **Master of Science in Micro and Nanotechnology Department, Middle East Technical University** by,

Prof. Dr. Canan Özgen
Dean, Graduate School of **Natural and Applied Sciences** _____

Prof. Dr. Mürvet Volkan
Head of Department, **Micro and Nanotechnology** _____

Prof. Dr. Mürvet Volkan
Supervisor, **Chemistry Dept., METU** _____

Prof. Dr. Necati Özkan
Co-Supervisor, **Polymer Science and Technology Dept.,METU** _____

Examining Committee Members:

Prof. Dr. O. Yavuz Ataman
Chemistry Dept., METU _____

Prof. Dr. Mürvet Volkan
Chemistry Dept., METU _____

Prof. Dr. Necati Özkan
Polymer Science and Technology Dept., METU _____

Prof. Dr. Ceyhan Kayran
Chemistry Dept., METU _____

Dr. Murat Kaya
Chemistry Dept., METU _____

Date: 24.10.2011

I hereby declare that all information in this document has been obtained and presented in accordance with academic rules and ethical conduct. I also declare that, as required by these rules and conduct, I have fully cited and referenced all material and results that are not original to this work.

Name, Last name : Gülfem Aygar

Signature :

ABSTRACT

PREPARATION OF SILICA COATED COBALT FERRITE MAGNETIC NANOPARTICLES FOR THE PURIFICATION OF HISTIDINE-TAGGED PROTEINS

Aygar, Gülfem

M.Sc., Department of Micro and Nanotechnology

Supervisor: Prof. Dr. Mürvet Volkan

Co-supervisor: Prof. Dr. Necati Özkan

October 2011, 80 pages

The magnetic separation approach has several advantages compared with conventional separation methods; it can be performed directly in crude samples containing suspended solid materials without pretreatment, and can easily isolate some biomolecules from aqueous systems in the presence of magnetic gradient fields. This thesis focused on the development of new class of magnetic separation material particularly useful for the separation of histidine-tagged proteins from the complex matrixes through the use of imidazole side chains of histidine molecules. For that reason surface modified cobalt ferrite nanoparticles which contain Ni-NTA affinity group were synthesized. Firstly, cobalt ferrite nanoparticles with a narrow size distribution were prepared in aqueous solution using the controlled coprecipitation method. In order to obtain small size of agglomerates two different dispersants, oleic acid and sodium chloride, were tried. After obtaining the best dispersant and optimum experimental conditions, ultrasonic bath was used in order to decrease the size of agglomerates. Then, they were coated with silica and this was

followed by surface modification of these nanoparticles by amine in order to add functional groups on silica shell. Next, –COOH functional groups were added to silica coated cobalt ferrite magnetic nanoparticles through the NH_2 groups. After that Nα,Nα-Bis(carboxymethyl)-L-lysine hydrate, NTA, was attached to carboxyl side of the structure. Finally, nanoparticles were labeled with Ni (II) ions. The size of the magnetic nanoparticles and their agglomerates were determined by FE-SEM images, particle size analyzer, and zeta potential analyzer (zeta-sizer). Vibrational sample magnetometer (VSM) was used to measure the magnetic behavior of cobalt ferrite and silica coated cobalt ferrite magnetic nanoparticles. Surface modifications of magnetic nanoparticles were followed by FT-IR measurements. ICP-OES was used to find the amount of Ni (II) ion concentration that was attached to the magnetic nanoparticle.

Keywords: Magnetic nanoparticles, ferrites, cobalt ferrite nanoparticles, surface modification, magnetic separation

ÖZ

HİSTİDİNLE İŞARETLENMİŞ PROTEİNLERİN SAFLAŞTIRILMASI İÇİN SİLİKA KAPLI MANYETİK KOBALT FERRİT NANOPARÇACIKLARININ HAZIRLANMASI

Aygar, Gülfem
Yüksek Lisans, Mikro ve Nanoteknoloji Bölümü
Tez Yöneticisi: Prof. Dr. Mürvet Volkan
Ortak Tez Yöneticisi: Prof. Dr. Necati Özkan

Ekim 2011, 80 sayfa

Manyetik ayırma yönteminin, bilinen ayırma yöntemleriyle kıyaslandığında, ön işlemden geçmemiş, askıda katı maddelerin bulunduğu ham örneğe, direkt olarak uygulanabilir olması ve bir çok biyomolekülün, manyetik alan etkisiyle sulu ortamdan kolayca izole edilmesi gibi bir çok avantaja sahiptir. Bu tezde, gelişmekte olan manyetik ayırma birimlerinin, histidinle işaretlenmiş proteinlerin, kompleks matriksten, histidin zincirinin imidazol tarafından, ayrılmasına değinilmiştir. Bu nedenle, Ni-NTA afinite grupları içeren, yüzeyi modifiye edilmiş kobalt ferrit nanoparçacıkları sentezlenmiştir. İlk olarak, sulu çözeltide, kontrollü birlikte çöktürme metoduyla, sınırlı boyut dağılımı olan kobalt ferrit nanoparçacıkları sentezlenmiştir. Küçük boyutta agglomeratlar elde etmek amacıyla, iki farklı dispersant, oleik asit ve sodyum klörür, denenmiştir. En uygun dispersant bulunduktan ve optimum koşullar sağlandıktan sonra, agglomeratların boyutlarını düşürmek için ultrasonik banyo kullanılmıştır. Daha sonra parçacıklar silikayla kaplanmıştır ve bu işlem, silika kabuğuna fonksiyonel gruplar eklenmesi için,

nanoparçacıkların yüzeylerine amin modifiye edilmesiyle devam etmiştir. Bunun ardından, silika kaplı kobalt ferrit nano parçacıklarına -NH_2 gruplarından, -COOH fonksiyonel grupları eklenmiştir. Bu işlemden sonra Nα,Nα-Bis(karboksimetil)-L-lysine hidrat, NTA, yapıya karboksil uçlarından eklenmiştir. Son olarak nanoparçacıklar, Ni (II) iyonlarıyla işaretlenmişlerdir. Manyetik nanoparçacıkların ve agglomeratların boyutları, FE-SEM görüntüleri, parçacık boyut analizi ve zeta potansiyel analizi ile belirlenmiştir. Kobalt ferrit ve silika kaplı kobalt ferrit manyetik nanoparçacıkların manyetik özellikleri, titreşimli örnek manyetometrisi (VSM) kullanılarak ölçülmüştür. Manyetik nanoparçacıkların yüzey modifikasyonları FT-IR ile izlenmiş ve manyetik nanoparçacığa tutturulan Ni (II) iyon konsantrasyonu ICP-OES kullanılarak bulunmuştur.

Anahtar Kelimeler: Manyetik nanoparçacık, ferritler, kobalt ferrit nanoparçacıklar, yüzey modifikasyonu, manyetik ayırma

To My Family,

ACKNOWLEDGEMENTS

I would like to express my sincere gratitude and thanks to my supervisor Prof. Dr. Mürvet Volkan for encouraging me to study in this area, giving patient guidance and providing great support throughout this thesis. It has been a great opportunity and pleasure to be a member of Prof. Volkan's group.

I would like to thank my co-supervisor, Prof. Dr. Necati Özkan for his guidance.

I have benefited a great deal from the experience and knowledge of Dr. Murat Kaya throughout this thesis. I thank to him for having an answer to all my questions.

I would like to thank Dr. Seher Karabıçak, for sharing her experience with me and for very valuable friendship.

I would like to thank Zeynep Ergül and Elif Kanbertay for their great friendship and support. We have lots of memories that will never be forgotten.

I would like to thank Tuğba Nur Aslan, Yeliz Akpınar, Dilek Ünal, Zehra Tatlıcı, Ceren Uzun, Lütfiye Sezen Keser, Bahar Köksal and Üzeyir Doğan for their great friendship, support and help in every situation.

I would like to thank Emrah Yıldırım for his help and friendship.

Endless thanks to my family, Sevim Aygar, Alparslan Aygar and Alper Aygar for their assets, love, trust and patience. They gave me endless love, believe me and support me in every situation.

TABLE OF CONTENTS

ABSTRACT iv

ÖZ vi

ACKNOWLEDGEMENTS ix

TABLE OF CONTENTS x

LIST OF FIGURES xiv

LIST OF TABLES xvii

CHAPTER 1

1. INTRODUCTION 1

1.1 Nanotechnology and Nanoparticles 1

1.2 Magnetic Nanoparticles 2

1.2.1 Magnetism and Magnetic Properties 3

1.2.2 Classification of the Magnetic Materials 7

1.2.2.1 Diamagnetism 7

1.2.2.2 Paramagnetism 8

1.2.2.3 Ferromagnetism 9

1.2.2.4 Antiferromagnetism 9

1.2.2.5 Ferrimagnetism 10

1.2.2.6 Superparamagnetism 12

1.3 Ferrites 13

1.3.1 Cobalt Ferrites 15

1.4 Synthesis of Magnetic Nanoparticles 16

1.4.1 Co-precipitation Method 17

1.5 Surface Coating of Magnetic Nanoparticles 18

1.5.1 Stabilization by Organic Coatings 18

1.5.2 Stabilization by Silica Coating 19
1.5.3 Functionalization of Coated Magnetic Nanoparticles 20
1.6 Applications of Magnetic Nanoparticles 21
1.6.1 Biomedical Applications 22
1.6.1.1 Magnetic Separation 23
1.7 Aim of the Study 26
2. EXPERIMENTAL 27
2.1 Chemical Reagents 27
2.1.1 Preparation of Cobalt Ferrite Magnetic Nanoparticles 27
2.1.2 Silica Coating on Cobalt Ferrite Magnetic Nanoparticles 27
2.1.3 Functionalization of Cobalt Ferrite Magnetic Nanoparticles with –NH_2 Groups 28
2.1.4 Attachment of –COOH (Carboxyl) Group on Nanoparticles 28
2.1.5 Surface Modification of Cobalt Ferrite Magnetic Nanoparticles with NTA 28
2.1.6 Adding Ni (II) Ions on Surface Modified Cobalt Ferrite Magnetic Nanoparticles 28
2.2 Instrumentation 29
2.2.1 Field Emission Scanning Electron Microscope (FE-SEM) 29
2.2.2 Energy Dispersive X-ray Spectrometer (EDX) 30
2.2.3 Vibrating Sample Magnetometer (VSM) 30
2.2.4 Fourier Transform Infrared Spectroscopy (FTIR) 30
2.2.5 Inductively Coupled Plasma Optical Emission Spectrometer (ICP-OES) 30
2.2.6 Zeta Potential Measurements 31

2.3 Preparation of Surface Modified Cobalt Ferrite Magnetic Nanoparticles ……..31

2.3.1 Preparation of Cobalt Ferrite Magnetic Nanoparticles..... 31

2.3.1.1 Using Oleic Acid as a Surfactant..... 31

2.3.1.2 Using Sodium Chloride (NaCl) as a Dispersant..... 32

2.1.1 Synthesis of Cobalt Ferrite Nanoparticles in Ultrasonic Bath 33

2.1.2 Silica Coating on Cobalt Ferrite Magnetic Nanoparticles..... 34

2.1.3 Functionalization of Silica Coated Cobalt Ferrite Magnetic Nanoparticles with Amine Groups..... 35

2.1.4 Adding –COOH Functional Groups to Amine Modified Cobalt Ferrite Magnetic Nanoparticles..... 36

2.1.5 Surface Modification of Cobalt Ferrite Magnetic Nanoparticles with NTA ……...37

2.1.6 Adding Ni (II) Ions to the NTA modified Cobalt Ferrite Magnetic Nanoparticles 37

3. RESULTS AND DISCUSSION 38

3.1 Preparation of Cobalt Ferrite Nanoparticles 38

3.1.1 Preparation of Cobalt Ferrite Nanoparticles by Using Oleic Acid 39

3.1.2 Preparation of Cobalt Ferrite Magnetic Nanoparticles by Using Sodium Chloride as a Dispersant 47

3.1.3 Preparation of Cobalt Ferrite Nanoparticles in Ultrasonic Bath 53

3.2 Silica Coating of Magnetic Cobalt Ferrite Nanoparticles..... 56

3.3 Magnetic Behavior of the Prepared Particles 63

3.3.1 Magnetic Behavior of Cobalt Ferrite Nanoparticles 63

3.3.2 Magnetic Behavior of Silica Coated Cobalt Ferrite Nanoparticles..... 64

3.4 Addition of Amine and Carboxyl Functional Groups on Silica Coated Cobalt Ferrite Nanoparticles 67

3.5 NTA Modified Magnetic Cobalt Ferrite Nanoparticles 69

3.6 Attachment of Ni (II) Ions to NTA Modified Cobalt Ferrite Nanoparticles 72

4. CONCLUSION 74

REFERENCES 76

LIST OF FIGURES

FIGURES

Figure 1 Applications of nanotechnology. 1
Figure 2 Magnetic field lines representation of a bar magnet and the magnetic field lines of magnetic forces (Spaldin, 2003). 4
Figure 3 Representation of magnetic dipoles (Callister, 2007)..... 4
Figure 4 A typical hysteresis loop for a ferromagnet.. 5
Figure 5 Retentivity and coercivity points of a typical hysteresis loop. 6
Figure 6 Reducing the area inside the hysteresis loop from 7
Figure 7 Ordering of the magnetic dipoles of diamagnetic materials (Spaldin, 2003). 8
Figure 8 The order of the domains of (a) diamagnetic material and (b) paramagnetic material (Callister,2007) 8
Figure 9 Magnetic dipole moments of a ferromagnetic material when external magnetic field is zero (Spaldin, 2003). 9
Figure 10 The magnetic dipole moments of manganese oxide (a) and a general antiferromagnetic material (Callister, 2007). 10
Figure 11 A type of a hysteresis loop of a ferrimagnetic material. 11
Figure 12 A schematic views of a ferrimagnetic material's magnetic dipole moments. Dipole moments are not totally cancelled each other. 11
Figure 13 Hysteresis loop comparison of three types of magnetic materials. Each color represents one type. Blue one is ferromagnetic, green one paramagnetic and red one is superparamagnetic materials (Spaldin, 2003)..... 13
Figure 14 The tetrahedral (A) and octahedral (B) sites (Spaldin, 2003). 14
Figure 15 Schematic view of spin moments on octahedral and tetrahedral positions at cubic ferrite structure that crystallize in the inverse spinel structure (Jun, Seo, & Cheon, 2008). 15
Figure 16 Structure of oleic acid. 19

Figure 17 Biologically and chemically functionalized magnetic nanoparticles (Parton, De Palma, & Borghs, 2007). 20
Figure 18 Applications of magnetic nanoparticles. (Magnetic Resonance Imaging-MRI) (Lu, Salabas, & Schüth, 2007). 21
Figure 19 Size comparison of biological molecules at nanoscale (Patel, 2007). 22
Figure 20 The structures of (a) nitriloacetic acid (NTA) and (b) histidine. 24
Figure 21 The structure of Ni (II) - NTA modified magnetic nanoparticles..... 25
Figure 22 The structure of a six adjacent (6X) histidine-tagged protein. 25
Figure 23 Separation of histidine-tagged proteins (Lee, et al., 2006). 26
Figure 24 The experimental setup used for the production of cobalt ferrite nanoparticles. 32
Figure 25 The experimental setup used for the production of cobalt ferrite nanoparticles synthesis. 33
Figure 26 The experimental set up used for the production of cobalt ferrite nanoparticles with ultrasonic bath. 34
Figure 27 Synthesis of silica coated cobalt ferrite nanoparticles. 35
Figure 28 The experimental setup for production of $–NH_2$ and –COOH modified cobalt ferrite nanoparticles. 36
Figure 29 FE-SEM image of cobalt ferrite nanoparticles. 40
Figure 30 EDX result of cobalt ferrite nanoparticles. 41
Figure 31 A histogram of cobalt ferrite agglomerates (oleic acid). 43
Figure 32 FE-SEM image of cobalt ferrite nanoparticles. 46
Figure 33 FE-SEM image of cobalt ferrite nanoparticles. 48
Figure 34 FE-SEM images of cobalt ferrite nanoparticles at different scales, 500 nm and 100 nm. 49
Figure 35 An EDX result of cobalt ferrite nanoparticles. 51
Figure 36 A histogram of cobalt ferrite agglomerates (NaCl was used as a dispersant) 52
Figure 37 FE-SEM image of cobalt ferrite nanoparticles (In ultrasonic bath). 54
Figure 38 A histogram of cobalt ferrite nanoparticles that were synthesized in ultrasonic bath. 56

Figure 39 Synthesis of silica coated cobalt ferrite nanoparticles. 57
Figure 40 FE-SEM image of silica coated cobalt ferrite nanoparticles. 58
Figure 41 EDX results of silica coated cobalt ferrite magnetic nanoparticles. 60
Figure 42 A histogram of silica coated cobalt ferrite nanoparticles. 61
Figure 43 FT-IR results of (a) cobalt ferrite nanoparticles and (b) silica coated cobalt ferrite nanoparticles. 62
Figure 44 Magnetic behavior of cobalt ferrite nanoparticles after external magnetic field was applied (1.6T). 63
Figure 45 Hysteresis curve of cobalt ferrite nanoparticles recorded at 300K and at a maximum magnetic field of 2.2 Tesla 64
Figure 46 Magnetic behavior of silica coated cobalt ferrite nanoparticles, after external magnetic field (1.6T) applied. Particles were collected in 60 seconds. 65
Figure 47 Hysteresis curve of silica coated cobalt ferrite nanoparticles recorded at 300K and at a maximum magnetic field of 2.2 Tesla. 66
Figure 48 Functionalization of silica coated cobalt ferrite nanoparticles with (a) –NH_2 and (b) –COOH functional groups. 67
Figure 49 FTIR results of (a) –NH_2 modified and (b) –COOH functionalized cobalt ferrite nanoparticles. 68
Figure 50 The structure of NTA (Nα,Nα-Bis(carboxymethyl)-L-lysine hydrate). ... 70
Figure 51 Attachment of a NTA molecule to the –COOH free group on the surface of cobalt ferrite nanoparticle. 70
Figure 52 (a) FT-IR results of pure NTA and (b) NTA modified cobalt ferrite nanoparticles. 71
Figure 53 Structure of the NTA modified cobalt ferrite nanoparticles after Ni (II) ion attachment (Tural, Kaya, Özkan, & Volkan, 2008). 72
Figure 54 Calibration curve of nickel standard solution. 73

LIST OF TABLES

TABLES

Table 1 Summary of co-precipitation method (Lu, Salabas, & Schüth, 2007). 17
Table 2 The particle size results of cobalt ferrite primary nanoparticles..... 42
Table 3 The Polydispersivity index values from the DLS method versus homogeneity. 43
Table 4 The DLS (zeta sizer) results of the agglomerated cobalt ferrite nanoparticles. 45
Table 5 The particle size results of cobalt ferrite primary nanoparticles..... 47
Table 6 The particle size results of cobalt ferrite primary nanoparticles..... 50
Table 7 The DLS (zeta sizer) results of agglomerated cobalt ferrite nanoparticles. . 52
Table 8 The particle size results of cobalt ferrite primary nanoparticles prepared with ultrasonic bath. 55
Table 9 The DLS (zeta sizer) results of agglomerated cobalt ferrite nanoparticles prepared with ultrasonic bath. 55
Table 10 The particle size results of silica coated cobalt ferrite primary nanoparticles. 59
Table 11 The DLS (zeta sizer) results of silica coated- agglomerated cobalt ferrite nanoparticles. 61

CHAPTER 1

INTRODUCTION

1.1 Nanotechnology and Nanoparticles

Nanotechnology is the technology dealing with both single nano-objects and materials and devices based on them and with processes that take place in the nanometer range (Gubin, Koksharov, Khomutov, & Yu., 2005). Nanotechnology, a broad and interdisciplinary research field, involving engineering, chemistry, physiology, biology and more, has been growing exponentially in the past few years, showing great potential for several applications, (Jun, Seo, & Cheon, 2008) such as in materials development, biomedical sciences, electronics, optics, magnetism, energy storage, and electrochemistry (Figure 1) (Safarik & Safarikova, 2002).

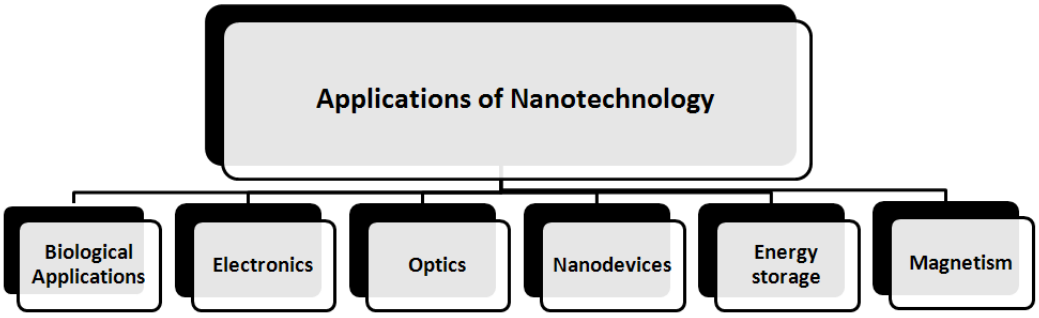

Figure 1 Applications of nanotechnology.

A particle with size between the range of 1 to 100 nm, at least in one of the three possible dimensions is called a ‘’nanoparticle’’. In this size range, the physical, chemical and biological properties of the nanoparticle change in fundamental ways from the properties of both individual atoms/molecules and of the corresponding bulk material (Nagarajan & Hatton, 2008). A typical well-known example is the fluorescence emission from semiconductor nanocrystals (quantum dots, QDs) which is dependent on the particle size and covers the entire visible spectrum. The number of atoms on surface increases with the decreasing the size of a particle (Shylesh, Schünemann, & Thiel, 2010).

Some examples of nanoparticles are; metals, metal oxides, silicates, non-oxide ceramics, polymers, organics, carbon and biomolecules. Nanoparticles exist in several different structures such as spheres, cylinders, platelets and tubes (Nagarajan & Hatton, 2008).

1.2 Magnetic Nanoparticles

Magnetic nanoparticles which exhibit a variety of unique magnetic phenomena that are drastically different from those of their bulk counterparts, are attain significant interest since these properties can be advantageous for utilization in a variety of applications (Jun, Seo, & Cheon, 2008) including magnetic fluids, catalysis, bio-applications, magnetic resonance imaging and data storage. (Lu, Salabas, & Schüth, 2007).

The magnetic properties of nanoparticles are determined by many factors, the key of these including the chemical composition, the type of the crystal lattice, the particle size and shape, the morphology, the interaction of the particle with the surrounding matrix and the neighboring particles. By changing the size, shape, composition and structure of nanoparticles, the magnetic properties of the materials can be controlled (Gubin, Koksharov, Khomutov, & Yu., 2005).

1.2.1 Magnetism and Magnetic Properties

Magnetism is a phenomenon through which materials assert an attractive or repulsive force on other materials (Callister, 2007). External magnetic field that is applied to a material is shown by **H**. The response of the material after external magnetic field, H, is applied is called magnetic induction, **B**. The relations between B and H, are show the magnetic property of the materials. The cgs unit of B is gauss and the unit of H is Oe. SI unit of B is weber/ m^2, or Tesla (T) and H is ampere-turn per meter (A/m).

The formula of the magnetization is: **M= m/V.** M is the magnetization of the medium, m is the magnetic moment and V is volume. The cgs unit of ‘’m’’ is ‘’emu’’ and the ‘’volume is ‘’cm^3’’. SI unit of M is the same as that of H (A/m).

The relationship between the external magnetic field, magnetic induction and magnetization in SI unit is:

$$\mathbf{B}=\mu_o(\mathbf{H}+\mathbf{M}) \qquad (1.2.1.1.)$$

μ_o is the permeability of free space. The ratio of magnetic induction to external magnetic field is called the permeability. μ shows the permeability of materials to the magnetic field (Formula 1.2.1.2.).

$$\mu= \mathbf{B}/\mathbf{H} \qquad (1.2.1.2.)$$

Another property of a material is susceptibility, *X*. The formula of susceptibility is:

$$X=\mathbf{M}/\mathbf{H} \qquad (1.2.1.3)$$

The susceptibility indicates the response of the magnetic material to external magnetic field (Spaldin, 2003).

A closed circulation of electric current is formed magnetic forces. Figure 2 shows the magnetic field lines of magnetic forces around the current loop and the magnetic field lines of a bar magnet (Callister, 2007).

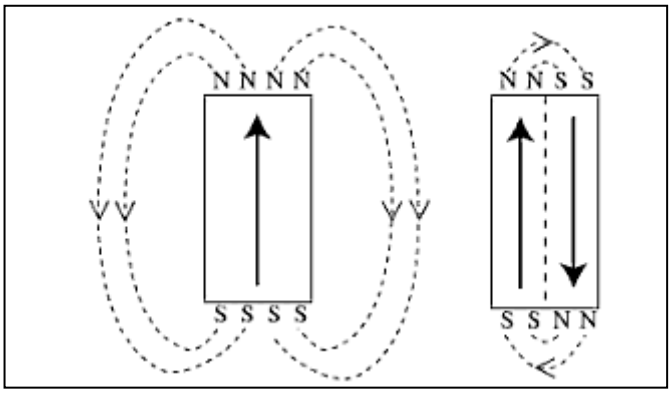

Figure 2 Magnetic field lines representation of a bar magnet and the magnetic field lines of magnetic forces (Spaldin, 2003).

Magnetic materials have magnetic dipoles that are represented the electric dipoles. Magnetic dipole moment show as an arrow (Figure 3). This arrow can be thought as a magnet which has a south and a north pole (Callister, 2007).

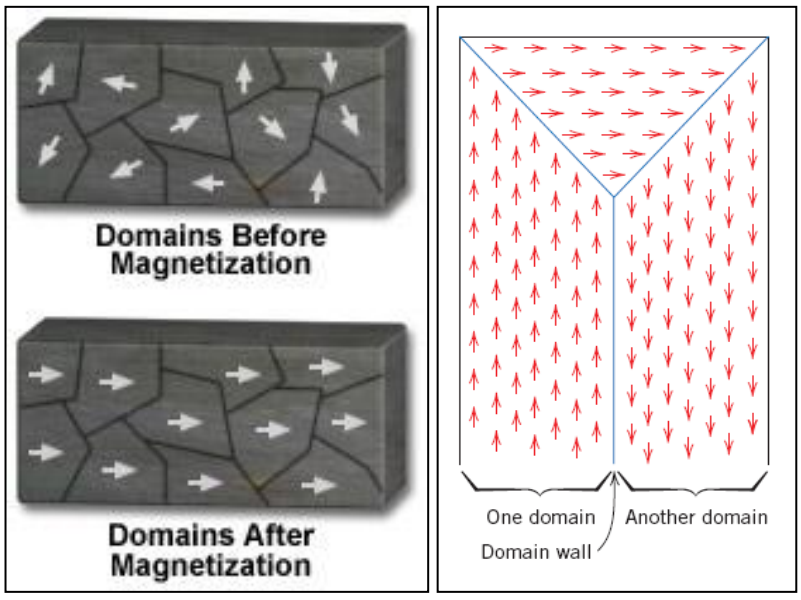

Figure 3 Representation of magnetic dipoles (Callister, 2007).

Domain walls separate the domains which have different directions (Figure 3). Domain (Bloch) walls are ~10μm in thickness (Spaldin, 2003). Each grain may have more than one domain. All domains have different magnetic orientation. The magnitude of magnetization, M, calculated by sum of all domain vectors. Sum of the domain vectors of non-magnetic material is zero (Callister, 2007).

When an external magnetic field is applied, the atomic dipoles align themselves with the external field. After the external field is removed, the magnetization value does not reduce to zero. The material has become magnetized. This phenomenon is called hysteresis. Figure 4 shows a typical ferromagnetic material's hysteresis loop. At saturation point, the maximum possible magnetization, or saturation magnetization of a ferromagnetic material is obtained. At this point all the magnetic dipoles in a solid material are aligned at the same direction with the external field.

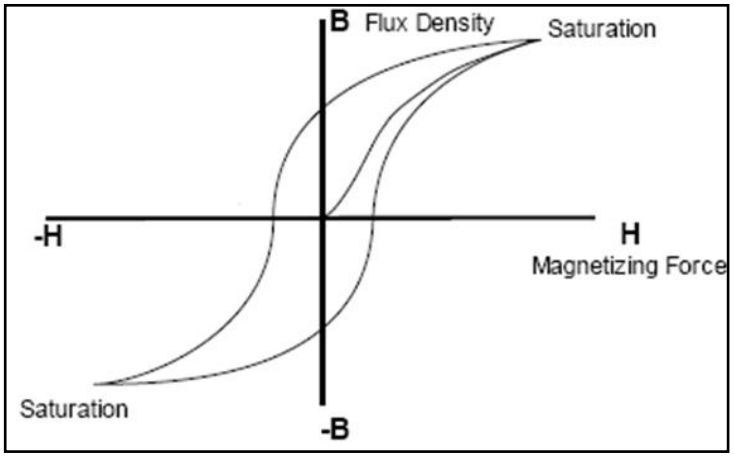

Figure 4 A typical hysteresis loop for a ferromagnet.

There are some important points at hysteresis loops, such as retentivity and coercivity (Figure 5). Coercivity is the point of the reverse field, required to lower the induction to zero value. Another one is retentivity point. When the external magnetic field removed, the saturation magnetization value does not reduce to zero. A certain amount of residual magnetic field retains, as a result, the material becomes permanent magnet (Spaldin, 2003).

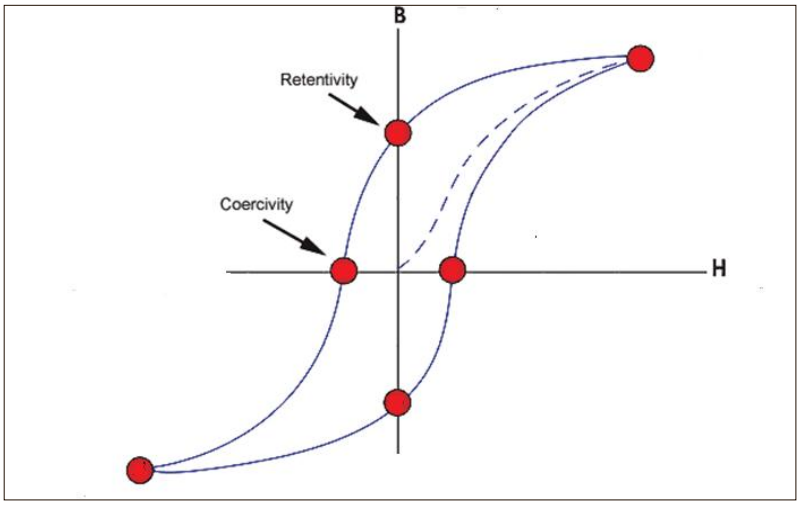

Figure 5 Retentivity and coercivity points of a typical hysteresis loop.

Ferromagnetic and ferrimagnetic materials are classified into two; hard or soft, depending of the coercivity values. A hard magnet needs a large field to reduce the induction to zero. It has high resistance to demagnetization (Callister, 2007). A soft magnet is easily saturated, but also easily demagnetized (Figure 6).

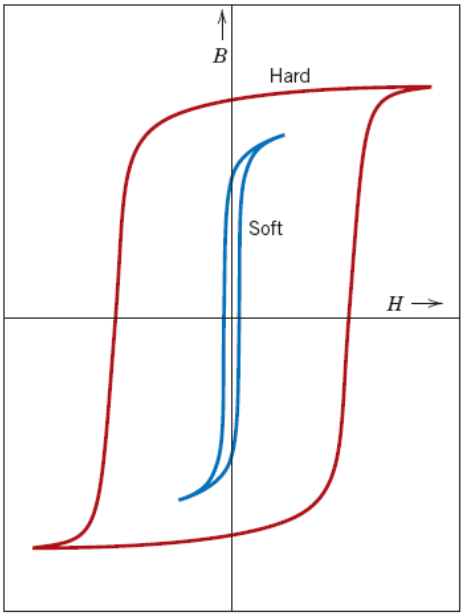

Figure 6 Reducing the area inside the hysteresis loop from hard magnet to soft magnet (Ralls, Courtney, & Wulff, 1976).

1.2.2 Classification of the Magnetic Materials

1.2.2.1 Diamagnetism

Magnetic materials that have diamagnetic properties are generated while the external magnetic field applied (Figure 8-a). It is very weak form of magnetism. The direction of magnetic dipole moments are opposite of the applied field, H (Figure 7). All materials have diamagnetic property because it is very weak. Diamagnetism can be observed if a magnetic material has no other type of magnetism. Diamagnetic materials are not used in so many applications as compared with other types of magnetism (Callister, 2007).

Magnetization of diamagnetic material decreases while the magnetic field increases because the susceptibility of a diamagnetic material is negative (Spaldin, 2003).

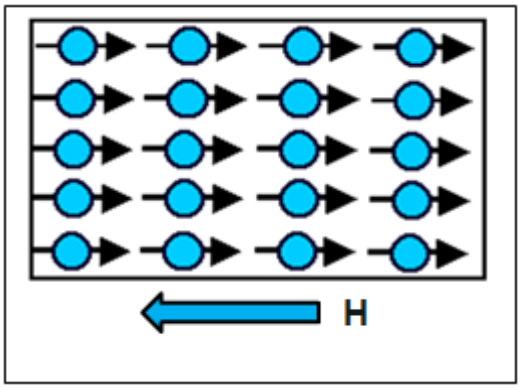

Figure 7 Ordering of the magnetic dipoles of diamagnetic materials (Spaldin, 2003).

1.2.2.2 Paramagnetism

Paramagnetic materials dipole moments have random orientation while the external magnetic field is zero. After magnetic field applied dipole moments align same direction through the applied magnetic field (Figure 8-b) (Callister, 2007).

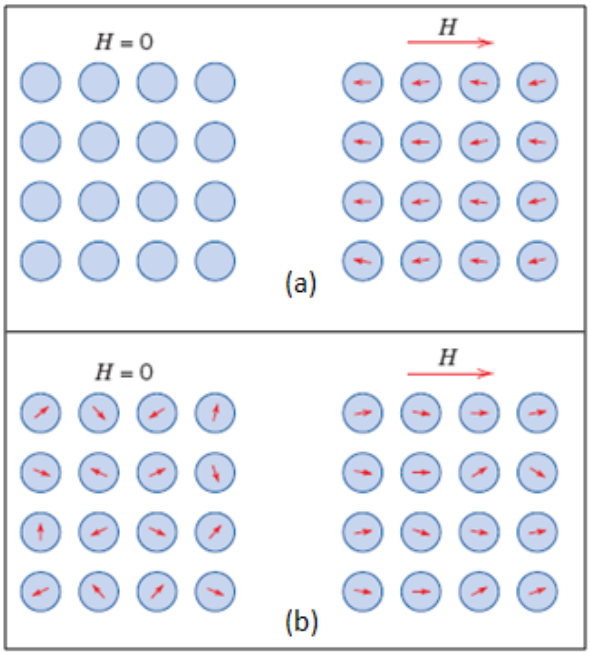

Figure 8 The order of the domains of (a) diamagnetic material and (b) paramagnetic material (Callister, 2007).

1.2.2.3 Ferromagnetism

Ferromagnetic materials show permanent magnetic property even if there is no external magnetic field. Figure 9 shows the magnetic dipole moments of ferromagnets which align in the same direction (Callister, 2007).

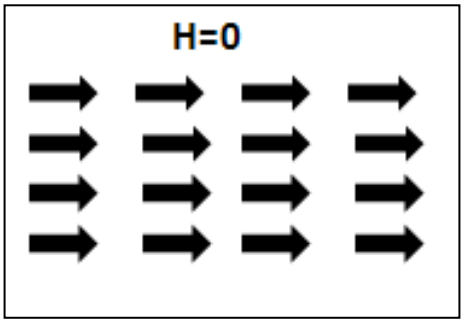

Figure 9 Magnetic dipole moments of a ferromagnetic material when external magnetic field is zero (Spaldin, 2003).

1.2.2.4 Antiferromagnetism

The spin moments of neighboring atoms are aligned opposite direction of each other. (Figure 10-a) Because of that these spin moments cancel each other. Net magnetization of antiferromagnetic materials is zero. Antiferromagnetic material such as manganese oxide at Figure 10 have manganese (Mn^{2+}) and oxygen (O^{2-}) ions. The magnetic dipole moments of Mn^{2+} ions cancel each other and no net magnetization occurs because of the cancellation. Net magnetic moment mainly comes from manganese ions. They arrange opposite of each other. Whole manganese oxide solid shows no net magnetic property (Callister, 2007).

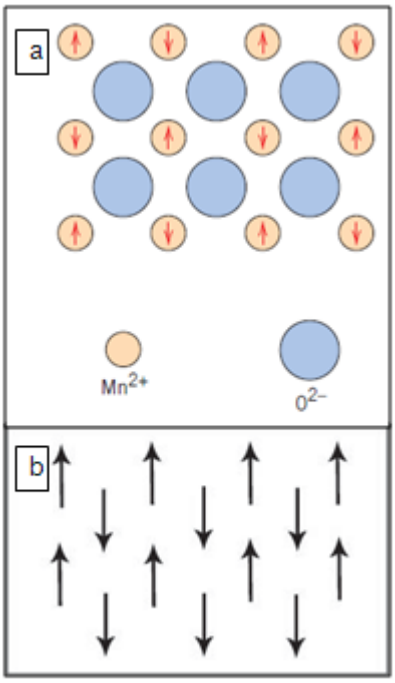

Figure 10 The magnetic dipole moments of manganese oxide (a) and a general antiferromagnetic material (Callister, 2007).

1.2.2.5 Ferrimagnetism

Ferromagnetism that have mentioned above and ferrimagnetism have similar magnetic characteristics. They have similar hysteresis loops (Figure11) Ferrimagnetic materials indicate permanent magnet property, absence of the external magnetic field.

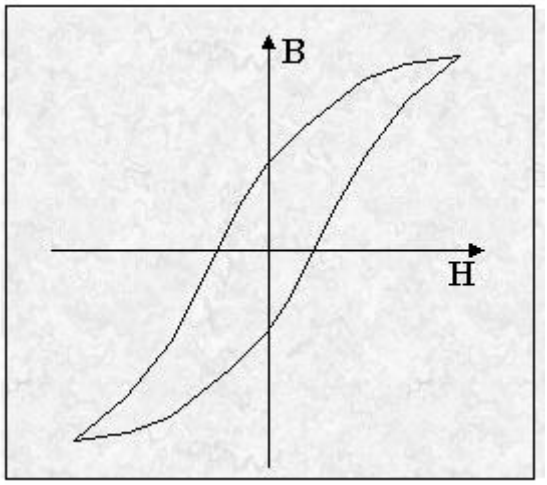

Figure 11 A type of a hysteresis loop of a ferrimagnetic material.

The magnetic dipole moments of a ferrimagnetic material are not totally canceling each other (Figure 12). Net magnetism occurs.

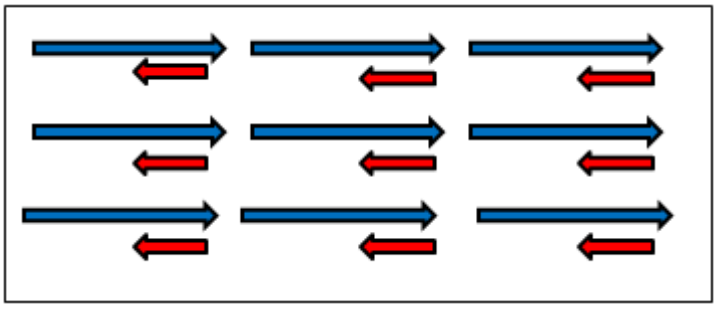

Figure 12 A schematic views of a ferrimagnetic material's magnetic dipole moments. Dipole moments are not totally cancelled each other.

Ferromagnetic materials have higher saturation magnetization values than ferrimagnetic materials (Spaldin, 2003).

1.2.2.6 Superparamagnetism

The hysteresis loop that are mentioned above have different shapes, depending on some properties ; such as, the sample single crystal or polycrystalline, orientation of crystalline sample , temperature and mechanical changes of the materials. Magnetic behavior on crystallographic orientation is defined as magnetic (magnetocrystalline) anisotropy (Callister, 2007).

The reverse field, coercivity decreases while the particle size radius decreases. Below 10 nm the coercivity becomes zero. This decrease of coercivity value result of an anisotropic energy reduction. The magnetic anisotropic energy is given by the product of the anisotropy constant, K, and the volume of the particle, V. The thermal energy k_BT can be comparable to the KV, while the volume decreases. Finally, the anisotropic energy is overcome by the thermal energy. Even the lack of external magnetic field, magnetization of particle change to one direction to another. This occurrence is called superparamagnetism. These small particles show same properties with the paramagnetic materials but they have higher saturation magnetization values.

Superparamagnetic material has no hysteresis loop like ferromagnetic materials. When the external magnetic field removed, its magnetization decreases to zero (Figure 13) (Spaldin, 2003).

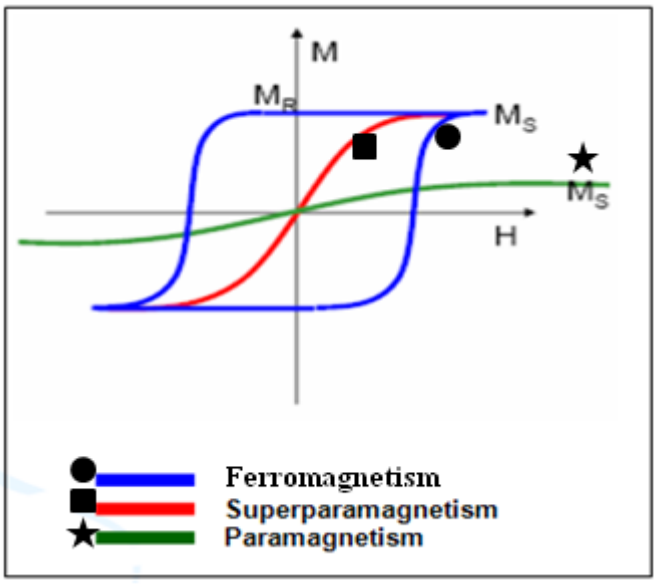

Figure 13 Hysteresis loop comparison of three types of magnetic materials. Each color represents one type. Blue one (●) is ferromagnetic, green one (★) paramagnetic and red one (■) is superparamagnetic materials (Spaldin, 2003).

1.3 Ferrites

Ferrite is a type of ferrimagnet. Ferrites are ferrimagnetic oxides and they are electrically insulating. Ferrites are widely used in high-frequency applications, because an AC field does not induce undesirable eddy currents in an insulating material (Callister, 2007), (Spaldin, 2003). Ferrites have two different structural symmetries which are determined by the size and charge of the metal ions that balance the charge of the oxygen ions, and their relative amounts (Goldman, 1990).

There are two types of ferrite. These are cubic and hexagonal ferrites. Cubic ferrites have a general chemical formula, MFe_2O_4. M represents the metallic elements, divalent ion (M^{2+}) ; such as, Mn^{2+} , Ni^{2+} , Fe^{2+} , Co^{2+} or Mg^{2+}. Cubic ferrites are soft magnetic materials. These ferrites crystallize in the normal or inverse spinel structure. If the $M^{2+,}$ divalent ions are on tetrahedral site A (Figure 14) and Fe^{3+} ions

are on B, octahedral sites, this type of material is in the normal spinel structure.

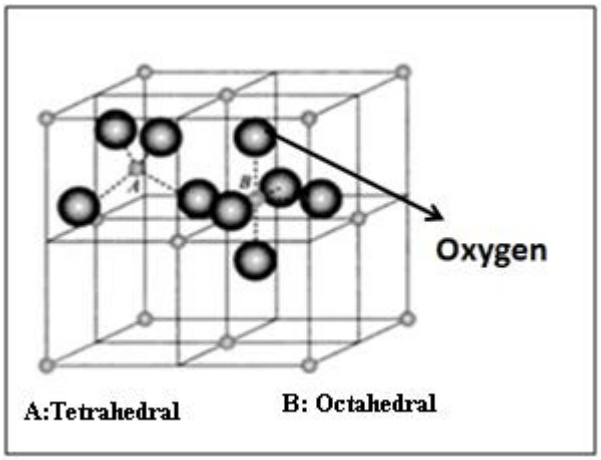

Figure 14 The tetrahedral (A) and octahedral (B) sites (Spaldin, 2003).

In the inverse spinels, some of B sites are occupied by divalent ions, and half of the Fe^{3+} ions are located A sites, the other half located B sites. At Figure 15 the green arrows (the direction of the arrows were also given) show the tetrahedral sites and the purple arrows show the octahedral sites. The spin moments of Fe^{3+} aligned both octahedral and tetrahedral sites. Effect of all Fe^{3+} ions cancel each other. Net magnetism is coming from divalent ion spin moments (Spaldin, 2003).

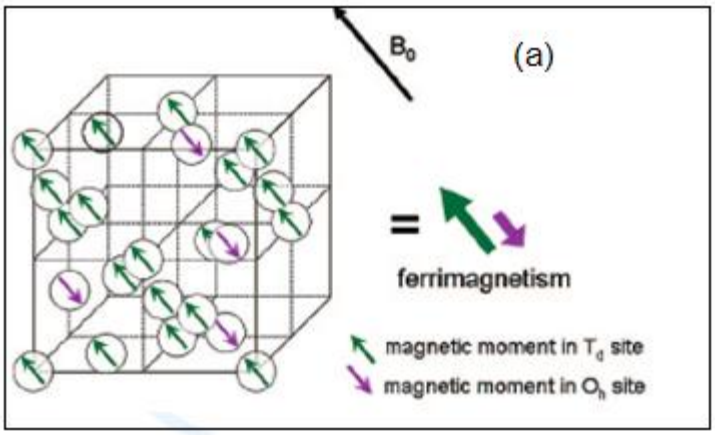

Figure 15 Schematic view of spin moments on octahedral and tetrahedral positions at cubic ferrite structure that crystallize in the inverse spinel structure (Jun, Seo, & Cheon, 2008).

Hexagonal ferrites are the inverse spinel structure. They have hexagonal symmetry. Their chemical formula is $AB_{12}O_{19}$. A represents a divalent metal (barium, lead, or strontium), and B represents the trivalent metal (aluminum, gallium, chromium, iron). $PbFe_{12}O_{19}$ and $BaFe_{12}O_{19}$ are the examples for hexagonal ferrites (Spaldin, 2003) .

Many groups have developed fabrication methods for magnetically stable ferrite nanoparticles, to achieve a fine-tuning of the size of ferrite nanoparticles employing different synthesis techniques and varying the experimental parameters such as heating rate, and quantity of surfactants including sonochemical reactions, sol-gel techniques, reverse micelles, host templates, coprecipitation, microemulsion procedures, thermal decomposition of organic complexes (precursor techniques), microwave, mechanochemical alloying, and hydrothermal or solvothermal routes (Jia, Chen, Jiao, He, Wang, & Jiang, 2008).

1.3.1 Cobalt Ferrites

Cobalt ferrite nanoparticles have important features such as their high magnetocrystalline anisotropy and large magneto-optical coefficients (Smit and Wijn 1959; Fontjin et al. 1999). Cobalt ferrite has a spinel structure (Gyergyek, Makovec, Kodre, Arcon, Jagodic, & Drofenik, 2009). It has a formula of $CoFe_2O_4$ ($CoO.Fe_2O_3$).

Cobalt ferrite, as a type of magnetic materials, has long been of intensive importance in the fundamental sciences and technological applications in various fields of electronics, photomagnetism, catalysis, ferrofluids, cancer therapy, and molecular imaging agents in magnetic resonance imaging (MRI). Cobalt ferrite is used in many applications because of its magnetic property. For biomedical applications, cobalt

ferrite nanoparticles are required to have a narrow size distribution, high saturation magnetization values, a homogeneous spherical shape, and superparamagnetic behavior at room temperature. The synthesis methods of cobalt ferrite nanoparticles are; hydrothermal, co-precipitation, micro emulsion and hydrolysis. The main problems of these methods are the particle size and shape cannot be control and agglomerated particles are formed. These situations limit their applications (Li, Xu, Han, Qiao, Wang, & Li, 2010).

Kim et al. prepared cobalt ferrite nanoparticles ranging from 2 to 14 nm by controlling co-precipitation temperature of cobalt ferrite ions in alkaline solution although the size distribution was pretty wide. Chinnasamy et al. employed a modified oxidation process to synthesize cobalt ferrite particles with diameters ranging from a few nanometers to about 15 nm. Rajendrain et al. demonstrated 6 to 20 nm sized cobalt ferrites prepared in aqueous solution at room temperature by the oxidative co-precipitation of cobalt ferrites. Morais et al. showed the size-controlled synthesis of the nanoparticles is 10 to 15 nm in aqueous solution at 95 ^{o}C by controlling stirring speed. Moumen et al. used oil-in-water micelle to prepare size-controlled cobalt ferrite in the range of 2 to 5 nm. Liu et al. also reported the nanoparticles of 2 to 35 nm in diameter which were prepared in normal micelle using similar method with the Moumen et al. Pillai et al. (Pillai & Shah, 1996). Sun et al., (Sun, et al., 2004) synthesized ferrite nanoparticles with sizes variable from 3 to 20 nm in diameter by combining non-hydrolytic reaction with seed-mediated growth method.

1.4 Synthesis of Magnetic Nanoparticles

Nanoparticles can be synthesized by a variety of methods using gas, liquid or solid phase processes. These include gas phase processes of flame pyrolysis, high temperature evaporation, and plasma synthesis; microwave irradiation; physical and chemical vapor deposition synthesis; colloidal or liquid phase methods in which chemical reactions in solvents lead to the formation of colloids; molecular self-assembly.

Mechanical processes of size reduction including grinding, milling and alloying (Nagarajan & Hatton, 2008). Magnetic nanoparticles have been synthesized various methods: thermal decomposition, micro emulsion (Lu, Salabas, & Schüth, 2007), hydrothermal, sonochemical, spray and laser pyrolysis, polyol (Tartaj, Morales, Veintemillas-Verdaguer, Gonzalez-Carreno, & Serna, 2003), and co-precipitation (Lu, Salabas, & Schüth, 2007).

1.4.1 Co-precipitation Method

Co-precipitation is a easy and useful way to synthesize iron oxides from aqueous Fe^{2+} /Fe^{3+} salt solutions by the addition of a base under inert atmosphere at room temperature or at elevated temperature. The size, shape, and composition of the magnetic nanoparticles depends on the type of salts used (e.g. chlorides, sulfates, nitrates), the Fe^{2+}/Fe^{3+} ratio, the reaction temperature, the pH value and ionic strength of the media (Lu, Salabas, & Schüth, 2007). Reaction temperature range, reaction time, solvent, size distribution, shape control and the yield of the method was given in Table 1.

Table 1 Summary of co-precipitation method (Lu, Salabas, & Schüth, 2007).

Synthesis Methods	**Co-precipitation**
Reaction Temp. °C	20-90
Reaction Time	Minutes
Solvent	Water
Size distribution	Relatively narrow
Shape Control	Not good
Yield	High

1.5 Surface Coating of Magnetic Nanoparticles

Nanoparticles tend to form agglomerates to reduce their energy. Because nanoparticles have high surface area to volume ratio. In addition, naked metallic nanoparticles are chemically highly active, and are easily oxidized in air. Consequently, magnetism decrease and they are not dispersed. It is not a desired situation, some protection methods apply to stabilize the naked magnetic nanoparticles against degradation during or after the synthesis. Protecting shells not only stabilize the nanoparticles, but can also be used for further functionalization (Lu, Salabas, & Schüth, 2007).

The coating types can be divided into two major groups: coating with organic shells, including surfactant and polymers, or coating with inorganic components, including silica, carbon, precious metals (such as Ag, Au) or oxides.

As an alternative, magnetic nanoparticles can also be dispersed/ embedded into a dense matrix, typically in polymer, silica, or carbon, to form composites, which also prevents or at least minimizes the agglomeration and oxidation (Lu, Salabas, & Schüth, 2007).

1.5.1 Stabilization by Organic Coatings

The aggregation of particles is avoided by using the amphiphilic capping agents such as long-chain fatty acids, diols, or alkyl amines. This is also useful to the regulation of size distribution. In order to adjust the stability, surfactants are used. Because of their dynamic adsorption and desorption characteristics, these materials helps to control the size, shape, magnetic, and chemical properties of nanoparticles. Nevertheless, their exchange properties are dependent to the strength and nature of the bond between the surfactant molecules and the nanoparticles. For example oleic acid (CH_3-$(CH_2)_7CH=CH(CH_2)_7COOH$), (Figure 16) , is commonly preferred to passivate iron oxides, because it can generate highly uniform and almost monodisperse nanocrystals (Shylesh, Schünemann, & Thiel, 2010).

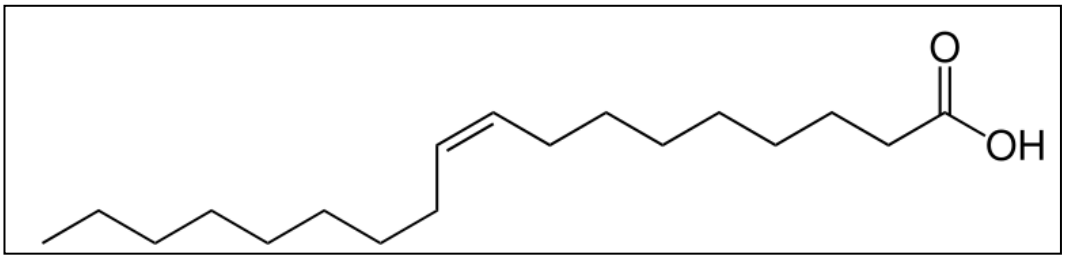

Figure 16 Structure of oleic acid.

1.5.2 Stabilization by Silica Coating

With the use of silica as coating material, more hydrophilic nanoparticles can be obtained which are more biocompatible than those produced by using oleic acid as stabilizing agent (Shylesh, Schünemann, & Thiel, 2010). The sol- gel technique is generally chosen to coat the magnetic nanoparticles. Silica is formed over the nanoparticles through the hydrolysis and condensation reaction of silicon alkoxides (typically, tetraethyl orthosilicate, TEOS) in alcohol/water mixtures under basic conditions as the Stöber method implies. In order to adjust thickness of the silica shell, reaction conditions can be altered. The use of silica shell aims to protect the magnetic cores and prevent the undesirable reactions (Lu, Salabas, & Schüth, 2007).

Silica coating prevents the agglomeration of cobalt ferrite magnetic nanoparticles. Because silica is not a magnetic material, it was decreases the particle-particle direct interaction. Furthermore, the hydrophilic surfaces of silica-coated magnetic nanoparticles can be modified with the functional groups. In addition, magnetic nanoparticles should be coated with silica layer before they were used in a biological application because silica was a nontoxic material (He, Wang, Li, Miao, Wu, & Zou, 2005).

1.5.3 Functionalization of Coated Magnetic Nanoparticles

A protective shell can be used for further functionalization with specific components, such as catalytically active species, various drugs, specific binding sites, or other functional groups (Lu, Salabas, & Schüth, 2007).

Silica-coated magnetic nanoparticles have additional advantages. It has –OH groups on surface, these groups were bonded to various functional groups; such as $–NH_2$, -COOH. These groups could not bond directly to the cobalt ferrite nanoparticles. Furthermore, the functionalization could introduce additional functionality, so that the magnetic particles can be used in biolabeling, drug targeting and drug delivery. Xia and co-workers have shown that commercially available ferrofluids can be directly coated with silica shells by the hydrolysis of tetraethyl orthosilicate,TEOS (Lu, Salabas, & Schüth, 2007). As can be seen from Figure 17, the functionalized silica surface, enabling chemical bonding of various fluorescent and biological species to the surface.

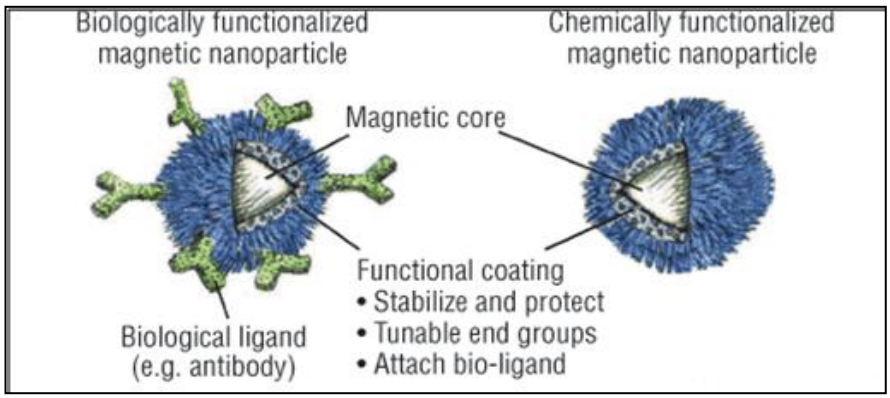

Figure 17 Biologically and chemically functionalized magnetic nanoparticles (Parton, De Palma, & Borghs, 2007).

1.6 Applications of Magnetic Nanoparticles

Depending on type of applications, magnetic nanoparticles are used in varieties of forms such as surface functionalized particles in biomedical applications, particles arrays in magnetic storage media, compacted powders in permanent magnets, and ferrofluids (Figure 18) (Berry & Curtis, 2003) , (Chinnasamy, Senoue, Jeyadevan, Perales-Perez, Shinoda, & Tohji, 2003).

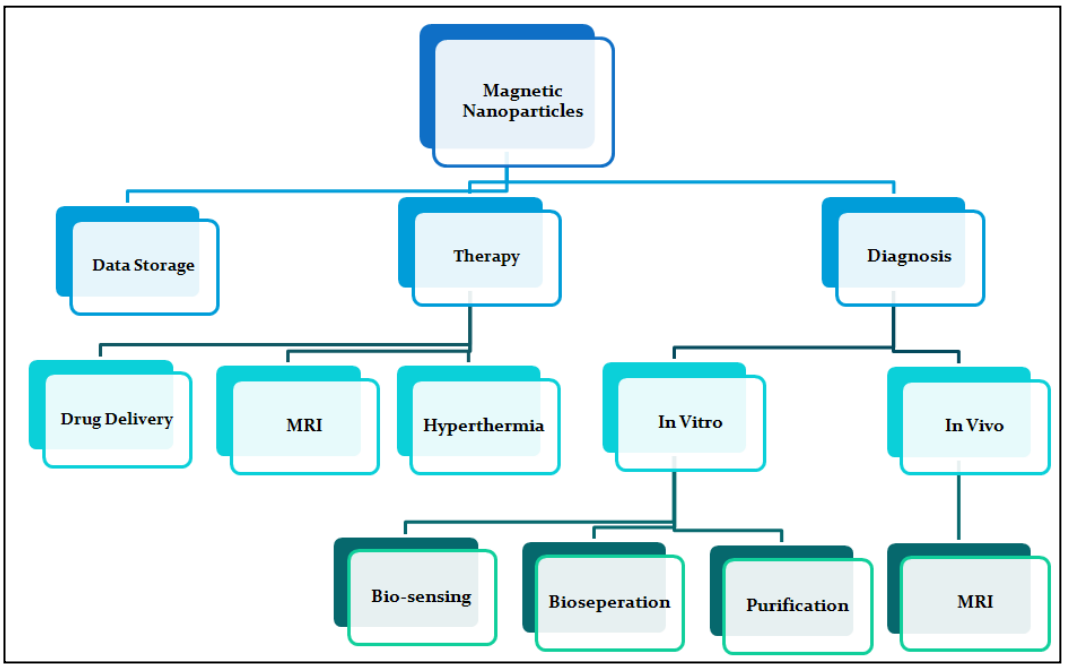

Figure 18 Applications of magnetic nanoparticles. (Magnetic Resonance Imaging-MRI) (Lu, Salabas, & Schüth, 2007).

1.6.1 Biomedical Applications

Magnetic nanoparticles have been proposed for biomedical applications for several years. In recent years, nanotechnology has developed to a stage that makes it possible to produce, characterize and specifically tailor the functional properties of nanoparticles for different applications. This shows considerable promise for applications in biomedical and diagnostic fields such as targeted drug delivery (Nagarajan & Hatton, 2008), hyperthermic treatment for malignant cell (De, Chosh, & Rotello, 2008), and magnetic resonance imaging (MRI). There are three reasons why the magnetic nanoparticles are useful in biomedical applications. First, magnetic nanoparticles can have controllable size ranging from a few nanometers up to tens of nanometers, and are smaller than comparable in sizes to a cell (10-100μm), a virus (20-450 nm), a protein (5 -50 nm) or a gene (2nm wide and 10 -100 nm long), Figure 19. They can get close to the cell or gene and they can be coated with biomolecules to make them interact or bind with biological entity.

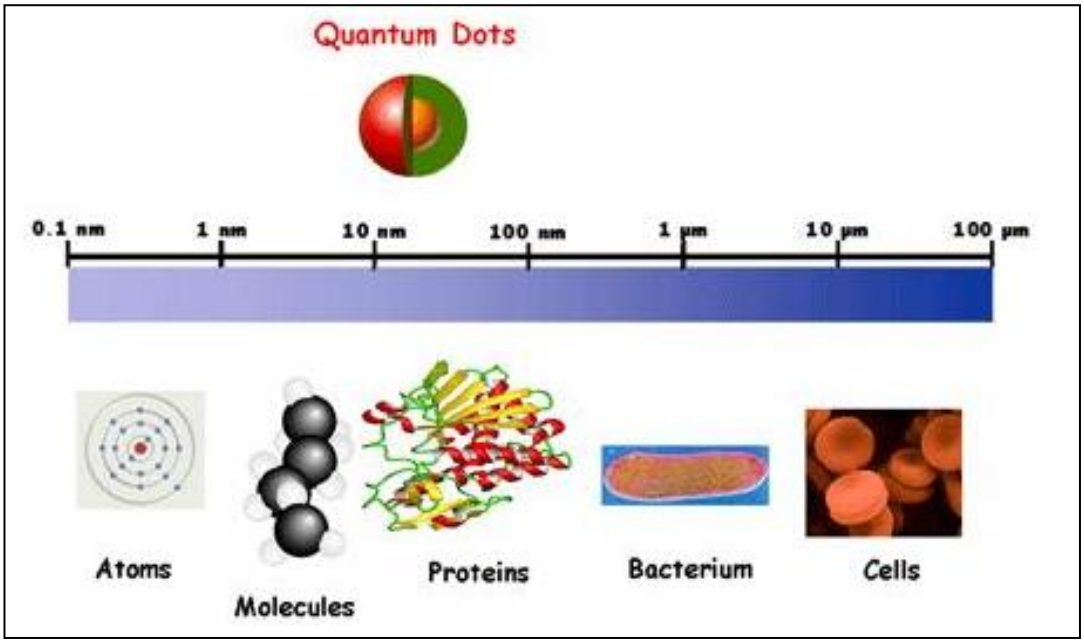

Figure 19 Size comparison of biological molecules at nanoscale (Patel, 2007).

Secondly, magnetic nanoparticles can be manipulated by an external magnetic field gradient. They can be used to deliver a package, such as an anticancer drug to a targeted region of the body such as a tumor. Third, magnetic nanoparticles can also be made to resonantly respond to a time-varying magnetic field, with an associated transfer of energy from the field to the nanoparticles. They can be made to heat up, which leads to their use as hyperthermia agents, delivering toxic amounts of thermal energy to targeted bodies such as tumors or as chemotherapy. As highlighted above for biomedical application, magnetic nanoparticles must (i) have a good thermal stability; (ii) have a larger magnetic moment; (iii) be biocompatible; (iv) be able to form stable dispersion so the particles could be transported in living system; and (v) response well to AC magnetic fields.

Furthermore, better control of particle size and properties will be necessary to use these particles in biomedical application, in which uniformity of the properties will ensure accurate dosing and delivery. The widely used magnetic nanoparticles for biomedical applications are magnetite (Fe_3O_4) and related oxides which are chemically stable, nontoxic, and non-carcinogenic and have attractive magnetic properties (Fu, Dravid, Klug, Liu, & Mirkin, 2002).

1.6.1.1 Magnetic Separation

Magnetic particles are widely used in the area of environmental, chemical and biomolecular industrial separations and reactions. Instead of traditional separation procedures, magnetic separation can be applied since it is more practical. For instance; it does not require expensive chromatography systems, it can be applied directly to crude samples containing suspended solid materials without pretreatment. It can also simply separate some biomolecules from aqueous systems in the presence of magnetic gradient fields (Liang, Zhang, & Jian, 2007). There is no need to apply centrifugation process. In addition, there isn't any risk of cross-contamination contrary to the traditional methods.

There are different types of magnetic particles which are commercially available for nucleic acid purification; magnetic separators working in the manual and automated mode are suggested (Berensmeier, 2006). The isolation of DNA or RNA is an important process before many biochemical and diagnostic treatment. Many downstream applications such as detection, cloning, sequencing, amplification, hybridization, cDNA synthesis, etc. cannot be carried out with the crude sample material. The presence of huge amounts of cellular or other contaminating substances, e.g. proteins or carbohydrates, in such complex mixtures often interferes with many of the subsequent reactions and techniques (Berensmeier, 2006).

Magnetic materials in nanoscale dimensions have been widely used for affinity isolation of proteins (Xu, et al., 2004), for capture and detection of bacteria at low concentration (Gu, Ho, Tsang, Wang, & Xu, 2003) and for separation of protein from biological samples (Bucak, Jones, Laibinis, & Hatton, 2003).

Xu and co-workers have synthesized functionalized magnetic nanoparticles with Ni (II)-NTA (NTA-nitrilotriacetic acid) complex (Figure 20-a) (Lee, et al., 2006). Nickel ions (Ni (II)) and some metals, such as cupper (Cu (II)), zinc (Zn (II)) and cobalt (Co (II)) ions have affinity for histidine (Tural, Kaya, Özkan, & Volkan, 2008). Histidine is a type of amino acid. The structure is shown below at Figure 20-b.

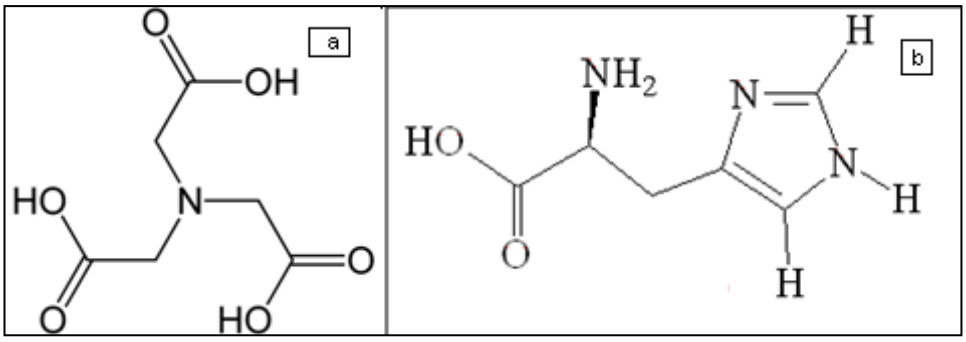

Figure 20 The structures of (a) nitriloacetic acid (NTA) and (b) histidine.

Ni (II)-NTA modified magnetic nanoparticles (Figure 21) bind to histidine-tagged proteins through the central metal ions.

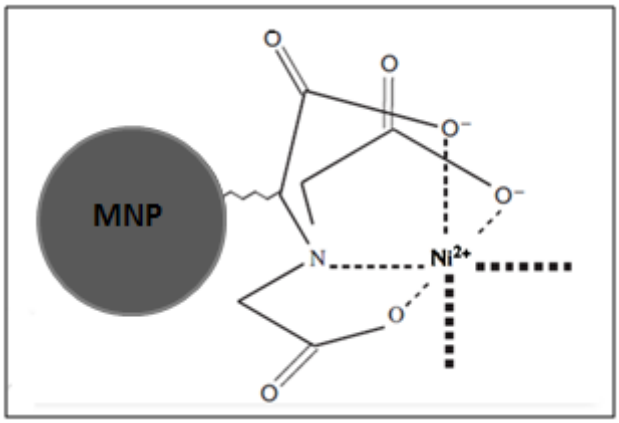

Figure 21 The structure of Ni (II) - NTA modified magnetic nanoparticles.

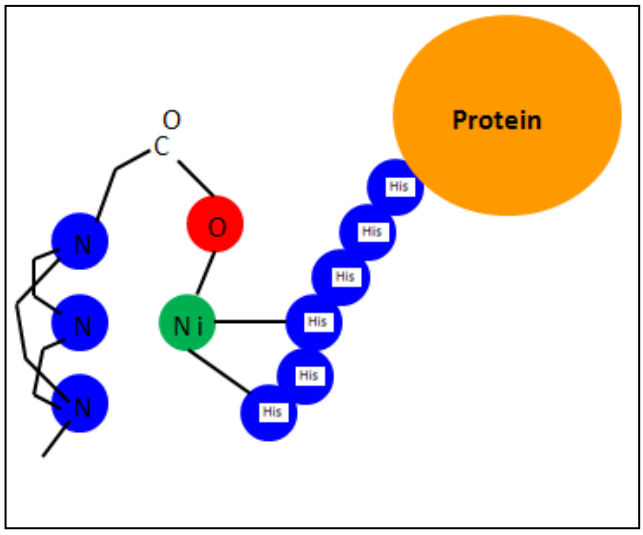

Figure 22 The structure of a six adjacent (6X) histidine-tagged protein.

This affinity type separation technique involves engineering a sequence of 6 to 8 histidines into the N- or C-terminal of the protein (Xu, et al., 2004) (Figure22). After magnetic field is applied, target histidine-tagged proteins are separated selectively from the medium (Figure 23) (Tural, Kaya, Özkan, & Volkan, 2008).

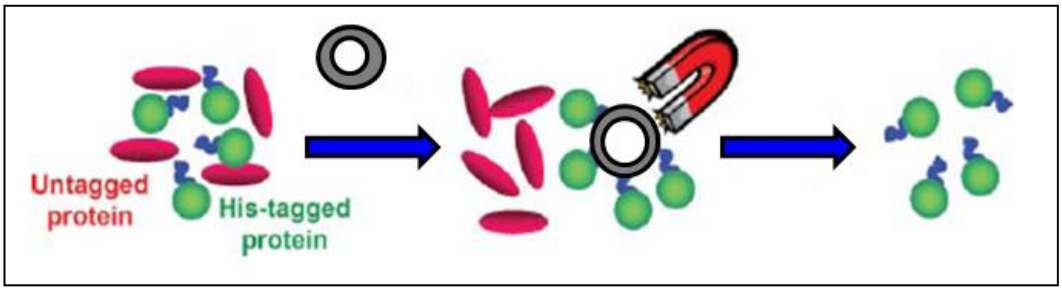

Figure 23 Separation of histidine-tagged proteins (Lee, et al., 2006).

1.7 Aim of the Study

The aim of this study is the preparation of surface modified cobalt ferrite magnetic nanoparticles as magnetic separation material for the magnetic separation of histidine-tagged proteins. For that reason, first cobalt ferrite magnetic nanoparticles were synthesized by using co-precipitation method. Then, the surface of magnetic nanoparticles were coated with silica and modified with Ni-NTA affinity group for histidine.

It is expected that histidine-tagged proteins could attach to the prepared cobalt ferrite nanoparticles having high magnetization and would be separated magnetically by applying external magnetic field.

CHAPTER 2

EXPERIMENTAL

2.1 Chemical Reagents

All chemicals and reagents were written in the order of their name, chemical formula, purity and manufacturer name.

2.1.1 Preparation of Cobalt Ferrite Magnetic Nanoparticles

i. **Iron(III)chloride,** $FeCl_3.9H_2O$, Riedel-de Haën

ii. **Cobalt(II) chloride 6-hydrate,** $CoCl_2.6H_2O$, Surechem

iii. **Sodium hydroxide pellets,** NaOH, Sigma-Aldrich

iv. **Sodium Chloride,** NaCl, Fisher Scientific Company

v. **Oleic acid, (9*Z*)-Octadec-9-enoic acid**, analytical standard, has been purchased from Fluka.

2.1.2 Silica Coating on Cobalt Ferrite Magnetic Nanoparticles

i. **Tetraethyl orthosilicate,** TEOS, $C_8H_{20}O_4Si$, 98%, Aldrich

ii. **(3-Aminopropyl)trimethoxysilane,** APTMS, $H_2N(CH_2)_3Si(OCH_3)_3$, ≥ 98.0%, Aldrich

iii. **Ethanol,** EtOH, C_2H_5OH, ≥ 99.9%, Merck

2.1.3 Functionalization of Cobalt Ferrite Magnetic Nanoparticles with $–NH_2$ Groups

i. **(3-Aminopropyl)triethoxysilane,** APTES, $C_9H_{23}NO_3Si$, ≥ 98.0%, Fluka

ii. **Toluene,** $C_6H_5CH_3$, ≥ 99.0%, Merck

iii. **N,N- Dimethylformamide,** DMF, C_3H_7NO, ≥ 99.8%, Sigma-Aldrich

2.1.4 Attachment of –COOH (Carboxyl) Group on Nanoparticles

i. **Toluene,** $C_6H_5CH_3$, ≥ 99.0%, Merck

ii. **N,N- Dimethylformamide,** DMF, C_3H_7NO, ≥ 99.8%, Sigma-Aldrich

iii. **Succinic (glutaric) anhydride,** $C_4H_4O_3$, ≥ 99%, Sigma- Aldrich

2.1.5 Surface Modification of Cobalt Ferrite Magnetic Nanoparticles with NTA

i. **Nα,Nα-Bis(carboxymethyl)-L-lysine hydrate,** NTA, $C_{10}H_{18}N_2O_6$, ≥ 97.0%, Fluka

ii. **2-(4-Morpholino)ethanesulfonic acid Potassium salt,** MES K salt, Sigma

2.1.6 Adding Ni (II) Ions on Surface Modified Cobalt Ferrite Magnetic Nanoparticles

i**. Nickel solution, Nickel (II) ion,** 1000 ppm ± 0.5%, Fisher Scientific International Company

All reagents used in this study were in analytical grade. De-ionized water was obtained from Millipore Milli-Q water deionization system. All the glass and plastic materials that were used at experimental procedures were cleaned by soaking in 10% HNO_3 at least for 1day and then rinsed with distilled water.

2.2 Instrumentation

2.2.1 Field Emission Scanning Electron Microscope (FE-SEM)

Quanta 400F Field Emission Scanning Electron Microscopy (FE-SEM (FEI)) located at METU Central Laboratory was used for morphological, spectroscopic characterization of cobalt ferrite and silica coated cobalt ferrite nanoparticles. For SEM measurements, the obtained suspension solution was dropped on carbon-coated copper grids and then they were dried at room temperature overnight.

Number-length (arithmetic) mean size (D[1,0]) and volume weighted mean size (D[4,3]) of cobalt ferrite and silica coated cobalt ferrite nanoparticles were determined from the FE-SEM images using the following formulas 2.2.1.1. and 2.2.1.2, respectively.

$$D[1,0]= \frac{\sum d_i N_i}{\sum N_i} \qquad \text{.....(2.2.1.1.)}$$

$$D[4,3] = \frac{\sum d_i^4 N_i}{\sum d_i^3 N_i} \qquad \text{.....(2.2.1.2.)}$$

'di' is the diameter of a nanoparticle and 'Ni' is the number of nanoparticles. In order to explain the calculations, imagine three spheres of diameters 1, 2 and 3 units. The average size of these three spheres are 2.00. It is calculated by summing all the diameters (Σd = 1 + 2 + 3) and dividing by the number of particles (n=3l). This is a number mean (number – length mean).The number-length mean size is also known as the arithmetic mean (Rawle, 2002).

2.2.2 Energy Dispersive X-ray Spectrometer (EDX)

SEM equipped with energy-dispersive X-ray analyzer (EDAX) at METU Central Laboratory was used for elemental analysis of cobalt ferrite and silica coated cobalt ferrite nanoparticles.

2.2.3 Vibrating Sample Magnetometer (VSM)

Saturation magnetization was measured with ADE Magneties Model EV9 Vibrating Sample Magnetometer at METU Metallurgical and Materials Engineering Department. The maximum field of VSM is 2.2 Tesla at room temperature.

2.2.4 Fourier Transform Infrared Spectroscopy (FTIR)

Alpha, Bruker model FTIR was used for characterization of nanoparticles in the range of 300 to 4500 cm^{-1}. FTIR (KBr pellet) analysis was performed at METU Analytical Chemistry Laboratory.

2.2.5 Inductively Coupled Plasma Optical Emission Spectrometer (ICP-OES)

Determination of Ni (II) ions attached on the surface modified cobalt ferrite nanoparticles were performed by ICP-OES (Direct Reading Echelle, Leeman Labs INC.) at METU Analytical Chemistry Laboratory.

Some of the parameters used in ICP-OES measurements were as follows: Incident plasma power was 1.2 kW, plasma coolant and the auxiliary Ar gas flow rates were set at 18 L/min and 0.5 L/min respectively. The nebulizer Ar was used at a pressure

of 50 psi. Peristaltic pump at 1.2 ml/min flow rate was used for sample transportation.

2.2.6 Zeta Potential Measurements

Particle size analysis of cobalt ferrite and silica coated cobalt ferrite nanoparticles were characterized by Malvern Nano ZS90 at METU Central Laboratory.

2.3 Preparation of Surface Modified Cobalt Ferrite Magnetic Nanoparticles

2.3.1 Preparation of Cobalt Ferrite Magnetic Nanoparticles

2.3.1.1 Using Oleic Acid as a Surfactant

At first part of the study, cobalt ferrite nanoparticles were synthesized by co-precipitation method (Peacock, 1966). 0.54 g $FeCl_3.6H_2O$, 0.238 g $CoCl_2.6H_2O$ and 10 ml deionized water were mixed in a test tube. The solution was put in a 50 ml beaker. During magnetic stirring, 10 ml 3 M NaOH was added dropwise with pasteur pipette, into that orange colored solution for 30 minute. After all NaOH aqueous solution was finished, 200 µl oleic acid was added to black precipitate colloid. The stirring was continued for 1 hour at 80^{o}C (Figure 24). After solution was cooled to room temperature, the black precipitates were collected with a magnet. Supernatant was removed and the particles were washed 3 times with deionized water –ethanol solution. Cobalt ferrite nanoparticles were redispersed in deionized water and stored in 15ml plastic tubes.

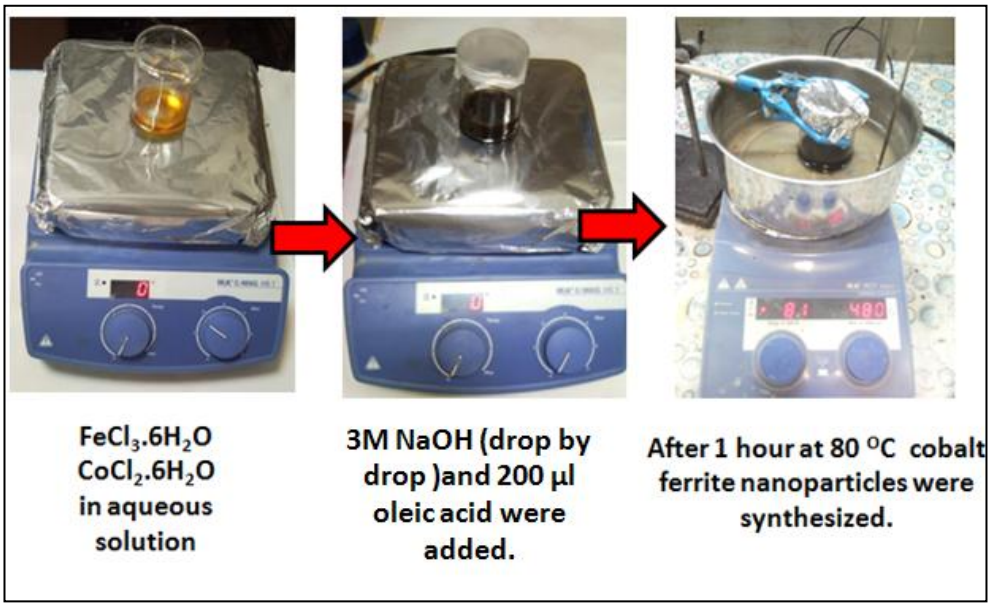

Figure 24 The experimental setup used for the production of cobalt ferrite nanoparticles.

2.3.1.2 Using Sodium Chloride (NaCl) as a Dispersant

Experimental procedure was shown in Figure 25. 0.54 g $FeCl_3.6H_2O$, 0.238 g $CoCl_2.6H_2O$ and 10 ml deionized water were vortexed in a tube. The solution was put in a 50ml beaker. During stirring on a magnetic stirrer, 10 ml 3 M NaOH and 5 ml 1.5 M NaCl added dropwise with pasteur pipettes into that orange colored solution for 30 minute. Stirring was continued for 1 hour at 80^{o}C. After solution was cooled to room temperature, the black precipitates were collected with a magnet. Supernatant was removed and the particles were washed 3 times with deionized water. Cobalt ferrite nanoparticles were stored in 15 ml plastic tubes in deionized water.

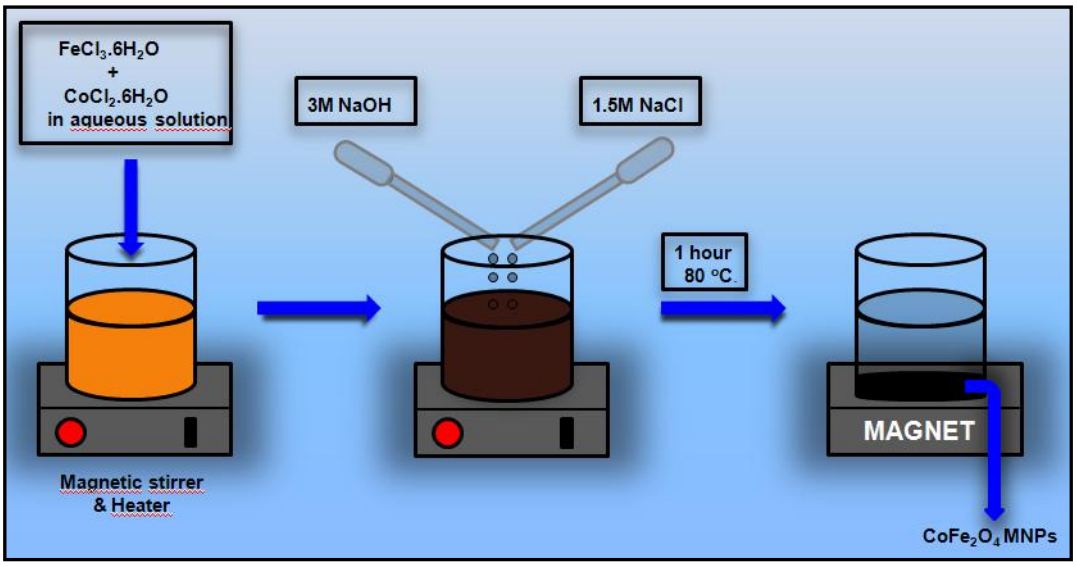

Figure 25 The experimental setup used for the production of cobalt ferrite nanoparticles synthesis.

2.1.1 Synthesis of Cobalt Ferrite Nanoparticles in Ultrasonic Bath

The same procedure, mentioned in section 2.3.1., was applied but at stirring step ultrasonic bath was used. Ultrasound was applied to the sample for 1 hour at 80^{o}C (Figure 26), and then solution was cooled to room temperature, the black precipitates were collected with a magnet. Supernatant was removed and the particles were washed 3 times with deionized water. Cobalt ferrite nanoparticles were stored in 15 ml plastic tubes in deionized water.

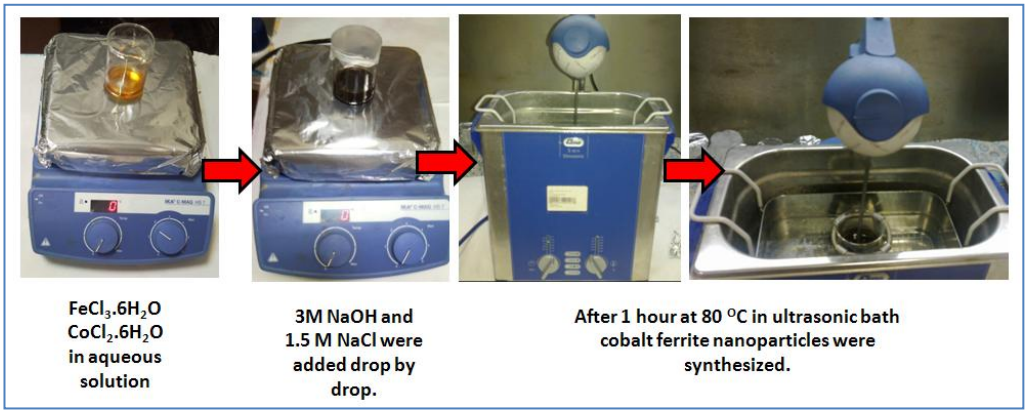

Figure 26 The experimental set up used for the production of cobalt ferrite nanoparticles with ultrasonic bath.

2.1.2 Silica Coating on Cobalt Ferrite Magnetic Nanoparticles

Cobalt ferrite magnetic nanoparticles were coated with silica shell by sol-gel method (Kobayashi, Horie, Konno, Rodriguez-Gonzales, & Liz-Marzan, 2003). First of all 80 ml ethanol, 169 µL TEOS and 14.4 µL APTMS were mixed in a beaker. 20 ml cobalt ferrite colloid was added to that solution and stirred for 3 hours at room temperature. After core shell particles were formed, these particles were collected with the magnet and washed three times with deionized water. Silica coated nanoparticles were stored in a 15 ml plastic tube. The schematic view of experimental procedure of silica coating on cobalt ferrite nanoparticles was given in Figure 27.

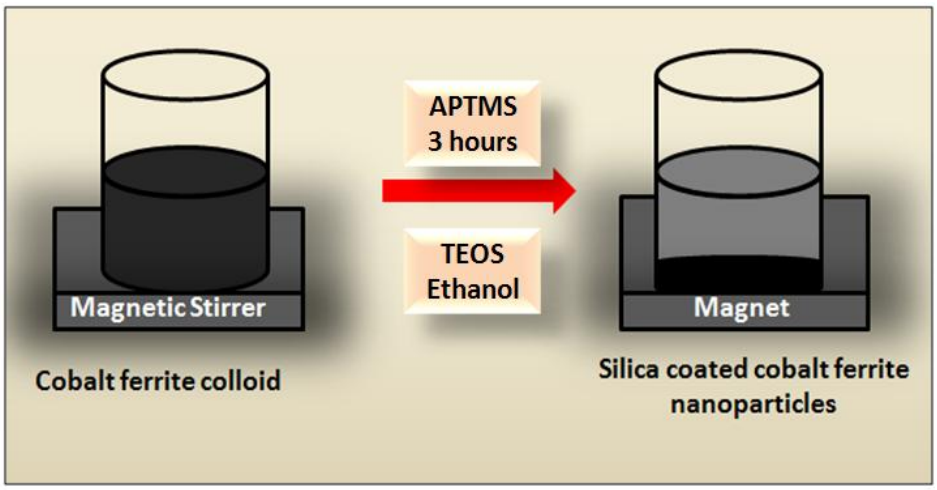

Figure 27 Synthesis of silica coated cobalt ferrite nanoparticles.

2.1.3 Functionalization of Silica Coated Cobalt Ferrite Magnetic Nanoparticles with Amine Groups

After silica shell was coated on the cobalt ferrite nanoparticle, the surfaces of these nanoparticles were modified with amine groups by APTES (He, Wang, Li, Miao, Wu, & Zou, 2005). At this process 12 ml DMF and 8 ml toluene were vortexed in a 50 ml tube and this solution was put in a 50 ml beaker. 200 µL APTES was added dropwise into that solution under magnetic stirring. Solution was mixed for 24 hour. After modifying the surface of cobalt ferrite nanoparticles with amine groups, these particles were collected with the magnet. And they were washed with toluene. Finally the nanoparticles were re-dispersed in 10 ml DMF in a 15 ml plastic tube. The experimental process was shown in Figure 28.

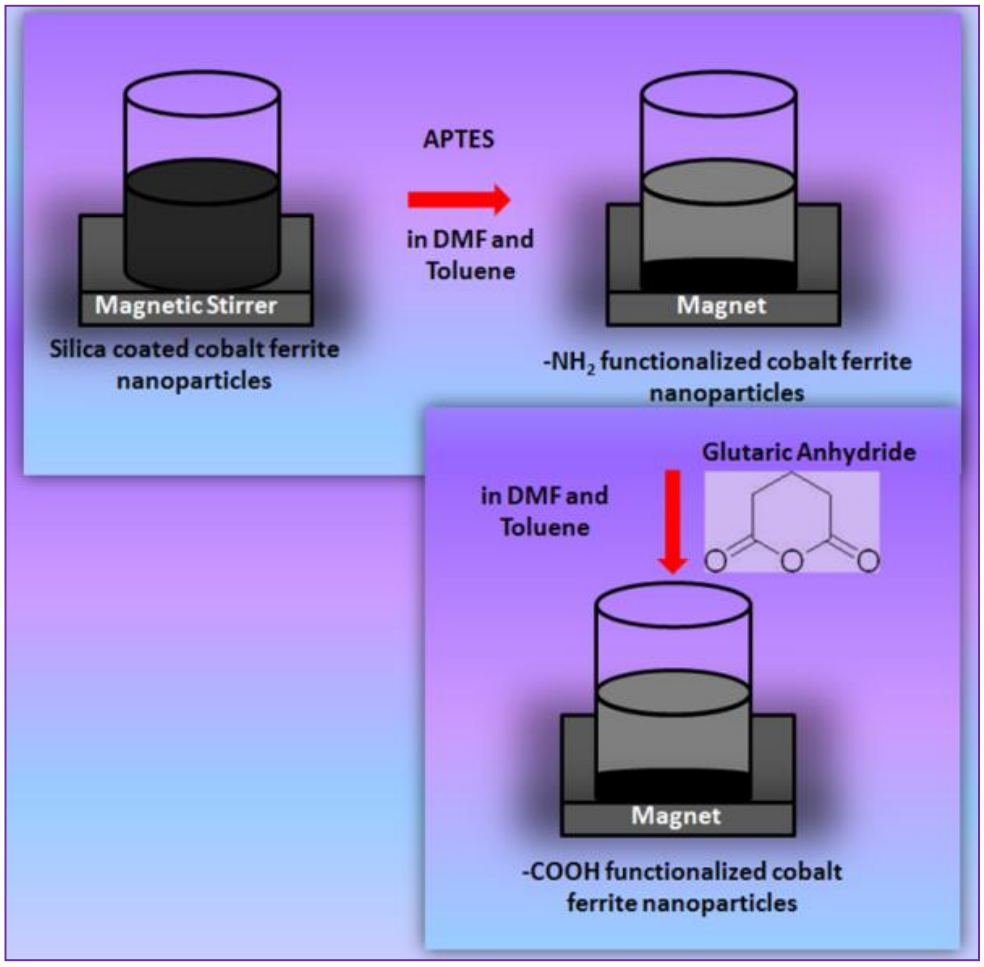

Figure 28 The experimental setup for production of –NH_2 and –COOH modified cobalt ferrite nanoparticles.

2.1.4 Adding –COOH Functional Groups to Amine Modified Cobalt Ferrite Magnetic Nanoparticles

10 ml DMF and –NH_2 modified cobalt ferrite nanoparticles were vortexed in a 15 ml plastic tube to make the colloid solution homogeneous. This solution was added dropwise to the solution that was 0.1 g glutaric anhydride in 10 ml DMF. This mixture was stirred with magnetic stirrer for 24 hour at room temperature. DMF was used to wash particles. All particles were separated from the washing medium, DMF and they were kept for other process. The experimental process was shown above in Figure 28.

2.1.5 Surface Modification of Cobalt Ferrite Magnetic Nanoparticles with NTA

5.8325 g MES K salt and 7.305 g NaCl were dissolved in 250 ml volumetric flask. The pH of the solution was adjusted to 6 with concentrated HCl. 7 ml solution was taken and mixed with 10 ml -COOH functionalized cobalt ferrite nanoparticles. 0.0787 g NTA was added to the solution and mixture was vortexed about 1 minute. The solution was put in a 50 ml beaker and stirred with magnetic stirrer for 2 hours. Nanoparticles were collected with the magnet and supernatant was removed. Particles were washed with deionized water.

2.1.6 Adding Ni (II) Ions to the NTA modified Cobalt Ferrite Magnetic Nanoparticles

1000 ppm nickel (II) ion solution diluted to the 20 ppm. 10 ml of 20 ppm Ni (II) ion solution were added to the –NTA modified particles. It was shaked slowly with shaker for 90 minute and all supernatant solution was taken. Particles were washed with 15 ml deionized water and supernatant was taken and combined with another supernatant. 25 ml supernatant solution was kept for ICP-OES measurements.

CHAPTER 3

RESULTS AND DISCUSSION

In this thesis, the synthesis of surface modified cobalt ferrite magnetic nanoparticles as magnetic separation unit in aqueous solution was reported. Co-precipitation based approach was used to produce cobalt ferrite nanoparticles. The effect of dispersants like oleic acid and sodium chloride on the size of formed cobalt ferrite nanoparticles and their agglomerates were investigated. After obtaining appropriate dispersant and optimum experimental conditions, effect of ultrasound application on the size of formed cobalt ferrite nanoparticles and their agglomerates was also investigated. Then Ni-NTA affinity groups were added by applying proper surface modifications.

3.1 Preparation of Cobalt Ferrite Nanoparticles

Cobalt ferrite nanoparticles, which have formulation of $CoFe_2O_4$, were synthesized by co-precipitation method (Maaz, Mumtaz, Hasanain, & Ceylan, 2007). The reactions regarding cobalt ferrite synthesis were given in the following equation.

$$CoCl_2.\ 6H_2O + 2FeCl_3.6H_2O + 8NaOH + n\text{NaCl} \rightarrow CoFe_2O_4 + (n + 8)\text{NaCl} + 16H_2O$$

In the preparation of magnetic nanoparticles, oleic acid and sodium chloride were used as dispersant. After obtaining appropriate dispersant and optimum experimental conditions, effect of ultrasound application on the size of formed cobalt ferrite nanoparticles and their agglomerates was investigated.

3.1.1 Preparation of Cobalt Ferrite Nanoparticles by Using Oleic Acid

In the first part of this study magnetic nanoparticles of cobalt ferrite have been synthesized by wet chemical method using stable ferric and cobalt salts with oleic acid as the surfactant as described in section 2.3.1.1. (Maaz, Mumtaz, Hasanain, & Ceylan, 2007). After obtaining the nanoparticles, washing process with ethanol and water was applied and precipitate was smashed and put in de-ionized water and it was vortexed. For FE-SEM measurement, 25µl colloid was taken and dropped on to carbon band. Then the structure of the produced cobalt ferrite nanoparticles was characterized by FE-SEM and EDX. FE-SEM was used to observe the morphology and the size distribution of the cobalt ferrite nanoparticles. Representative FE-SEM images and EDX patterns of prepared cobalt ferrite nanoparticles were shown in Figure 29 and Figure 30, respectively.

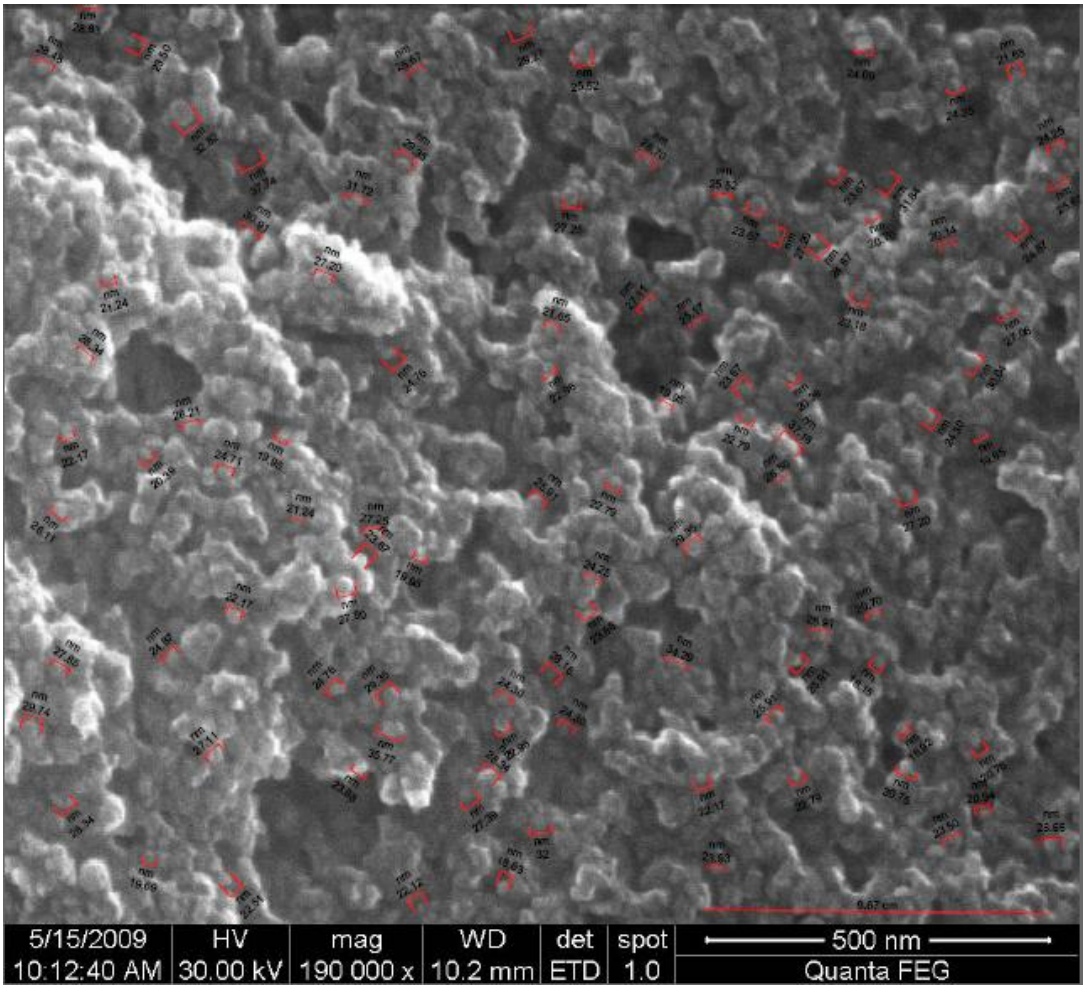

Figure 29 FE-SEM image of cobalt ferrite nanoparticles.

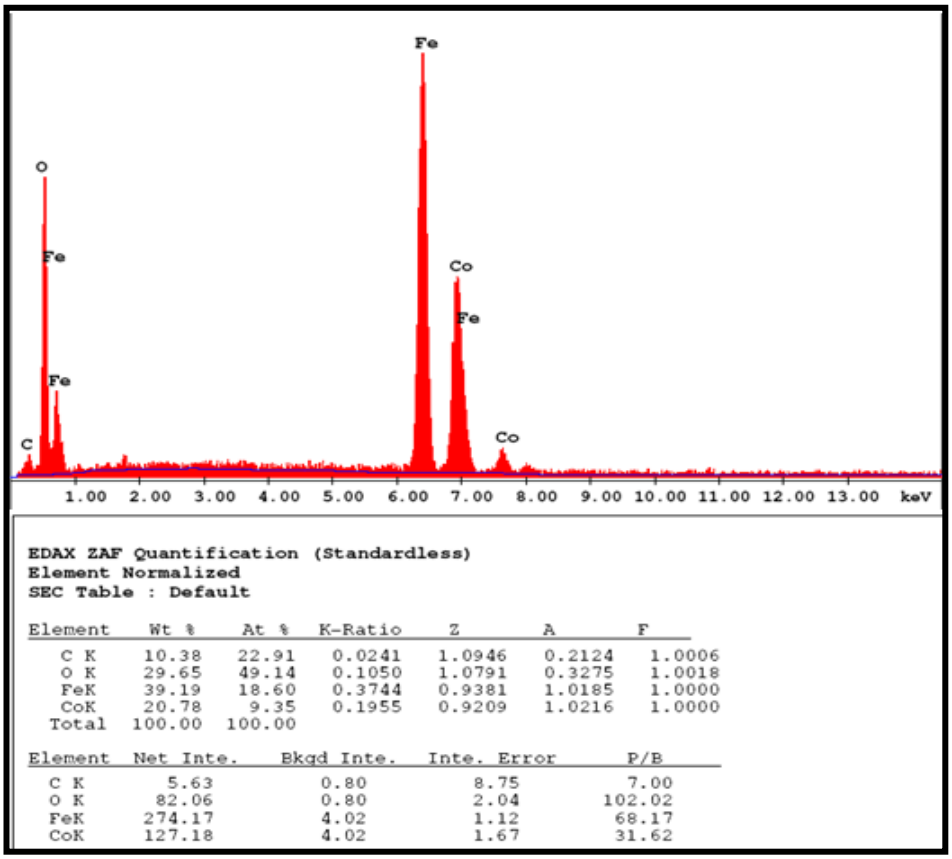

Figure 30 EDX result of cobalt ferrite nanoparticles.

From the FE-SEM image (Figure 30), randomly 100 particles were selected. The number-length (arithmetic) mean size (D[1,0]) and volume weighted mean size (D[4,3]) of primary cobalt ferrite nanoparticles was calculated from the formula 2.2.1.1. and 2.2.1.2. , respectively. The number-length mean size was calculated as 25.13 nm and the volume weighted mean size was calculated as 27.4 nm. At FE-SEM image, it was observed that excess oleic acid was not removed properly from the surface of the nanoparticles, therefore lots of agglomerated particles were coated with oleic acid and formed big clusters.

Polydispersivity index (PDI), which gives information about homogeneity, was calculated using the ratio of volume weighted mean size to number-length mean size. And this calculated PDI was different from the PDI, which was calculated from the dynamic light scattering (zeta sizer). The formula of PDI was given as;

$$PDI = \frac{D[4,3]}{D[1,0]} \qquad \text{..... (3.1.1.1.)}$$

Polydispersivity index of oleic acid coated cobalt ferrite nanoparticles was calculated as 1.09. Relatively homogeneous primary particle size distribution was obtained since the PDI value was close to 1.00 which represents mono size distribution. The particle size results, obtained using SEM pictures, were summarized in the following Table (Table 2).

Table 2 The particle size results of cobalt ferrite primary nanoparticles.

Primary $CoFe_2O_4$ particles	**Number-length mean size (nm) D[1,0]**	**Volume weighted mean size (nm) D[4,3]**	**Polydispersivity Index (PDI)**
Surfactant: Oleic acid	25.13	27.4	1.09

The size of the agglomerates was measured by using dynamic light scattering method (zeta sizer) to show particle size distribution trend. A histogram of agglomerated cobalt ferrite nanoparticles was given in Figure 31.

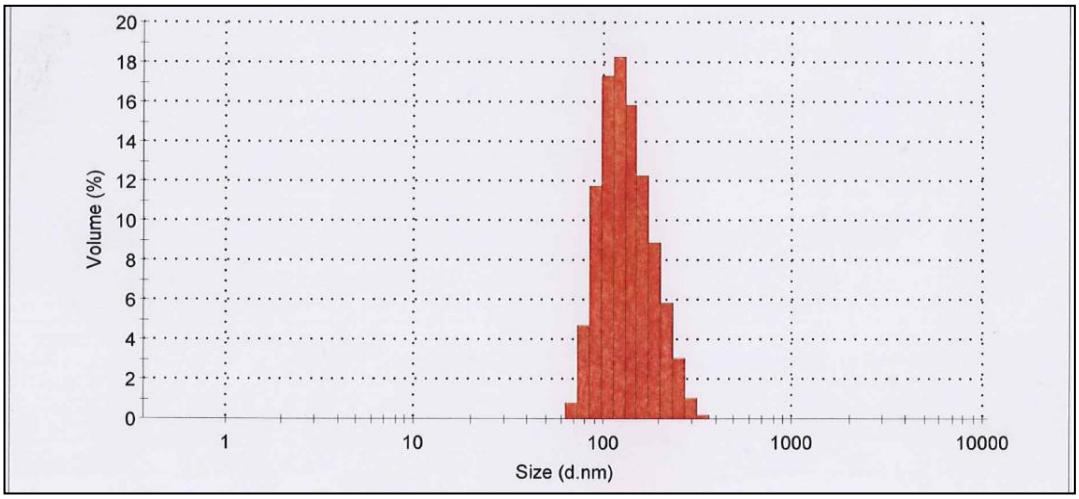

Figure 31 A histogram of cobalt ferrite agglomerates (oleic acid).

The z-average mean size of the cobalt ferrite agglomerates at pH ~7 was 147.4 nm. The size distribution of the particles was in the range of 70 and 350 nm. The PDI values gives information about homogeneity of cobalt ferrite agglomerates (Table 3).

Table 3 The Polydispersivity index values from the DLS method versus homogeneity.

Range of Polydispersivity Index Values	**Homogeneity of $CoFe_2O_4$ agglomerates**
0.00-0.05	Monodisperse
0.05-0.08	Nearly monodisperse
0.08- 0.7	Mid-range polydispersivity

The PDI of cobalt ferrite agglomerates (oleic acid) was given as 0.042. As shown in Table 3, nearly monodisperse agglomerate size distribution was obtained. The volume weighted mean size of cobalt ferrite agglomerates was calculated from the following formula 3.1.1.2.;

$$D[4,3]= \frac{\sum d_i V_i}{\sum V_i}$$

…….(3.1.1.2.)

'd*i*' was the size of a cobalt ferrite agglomerate and 'V*i'* was the volume fraction.

Specific Surface Area (S*v*) of cobalt ferrite agglomerates was calculated from the following formulas; 3.1.1.3. and 3.1.1.4 . The unit of specific surface area was given as m^2/g or m^2/cm^3;

$$D[3,2] = \frac{\sum d_i^3 N_i}{\sum d_i^2 N_i}$$

……..….(3.1.1.3.)

$$Sv = \frac{6}{D[3,2]}$$

…….....(3.1.1.4.)

From the data of histogram (Figure 31), the volume weighted mean size was calculated as 139.7 nm. And the specific surface area of cobalt ferrite agglomerates was calculated as 47.36 m^2/cm^3. All DLS (zeta sizer) results were given in Table 4.

Table 4 The DLS (zeta sizer) results of the agglomerated cobalt ferrite nanoparticles.

Agglomerated $CoFe_2O_4$ particles	Z-avarage mean size (nm)	Volume weighted mean size (nm)	Polydispersivity Index	Specific Surface Area (m^2/cm^3)
Surfactant: Oleic acid	147.4	139.7	0.042	47.36

In order to remove the excess oleic acid from the surface of the nanoparticle, the number of washing process with ethanol and water was increased. To examine whether a well dispersed nanoparticles was obtained after increasing the washing steps, FE-SEM images of the nanoparticles were taken as shown in Figure 32.

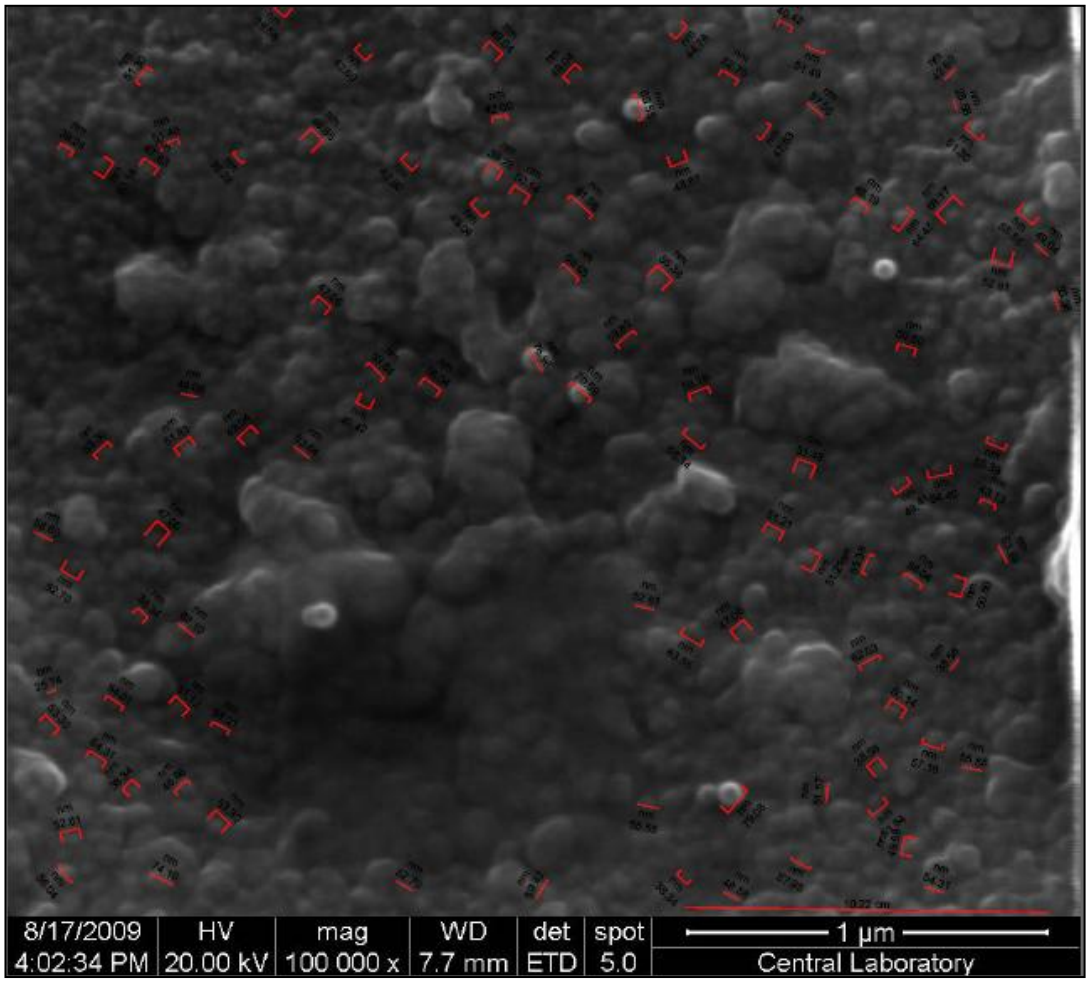

Figure 32 FE-SEM image of cobalt ferrite nanoparticles.

The number-length (arithmetic) mean size (D[1,0]) and volume weighted mean size (D[4,3]) of the primary cobalt ferrite nanoparticles from Figure 32 were calculated as, 52.08 nm and 57.4, respectively. The values were given in Table 5. The PDI value was 1.10. The observations suggested that increasing the washing steps did not help to decrease the amount of excess oleic acid covering the nanoparticle surfaces and leading to the formation of big agglomerate type structures.

Table 5 The particle size results of cobalt ferrite primary nanoparticles.

Primary $CoFe_2O_4$ particles	Number-length mean size (nm) D[1,0]	Volume weighted mean size (nm) D[4,3]	Polydispersivity Index (PDI)
Surfactant: Oleic acid	52.08	57.4	1.10

3.1.2 Preparation of Cobalt Ferrite Magnetic Nanoparticles by Using Sodium Chloride as a Dispersant

In order to resolve the above problem (in the case of oleic acid), a method for low temperature solid state synthesis of highly dispersive cobalt ferrite nanoparticles *via* introduction of inert soluble salt into the precursor mixture was tried.

In this work, a salt-assisted low temperature solid state method using $CoCl_2.6H_2O$, $FeCl_3.6H_2O$ and NaOH as precursor and using NaCl as a dispersant to synthesize high surface area cobalt ferrite nanoparticles has been investigated in order to obtain smaller particles and reduce agglomeration (Qin, Li, Jiang, & Liu, 2009). The FE-SEM image of cobalt ferrite nanoparticles is shown in Figure 33 and 34.

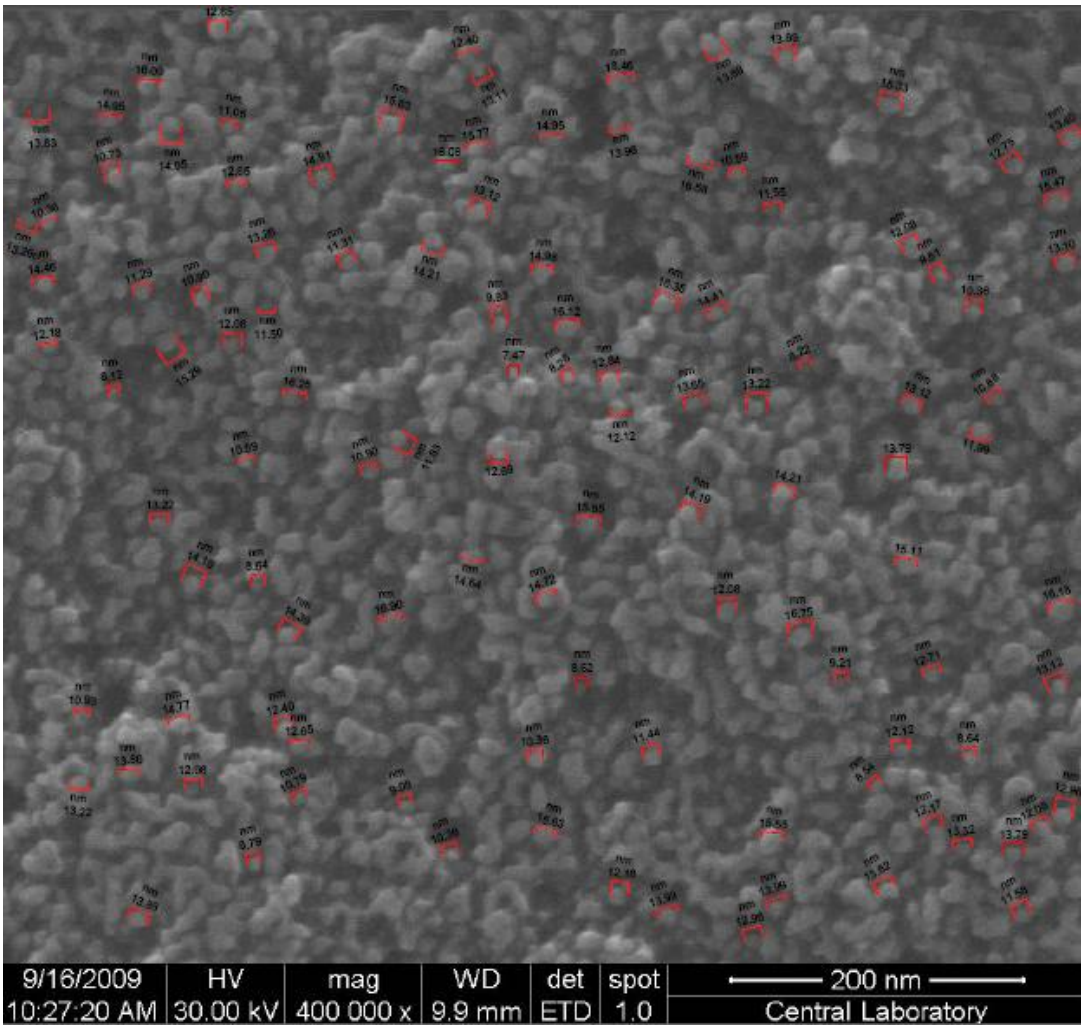

Figure 33 FE-SEM image of cobalt ferrite nanoparticles.

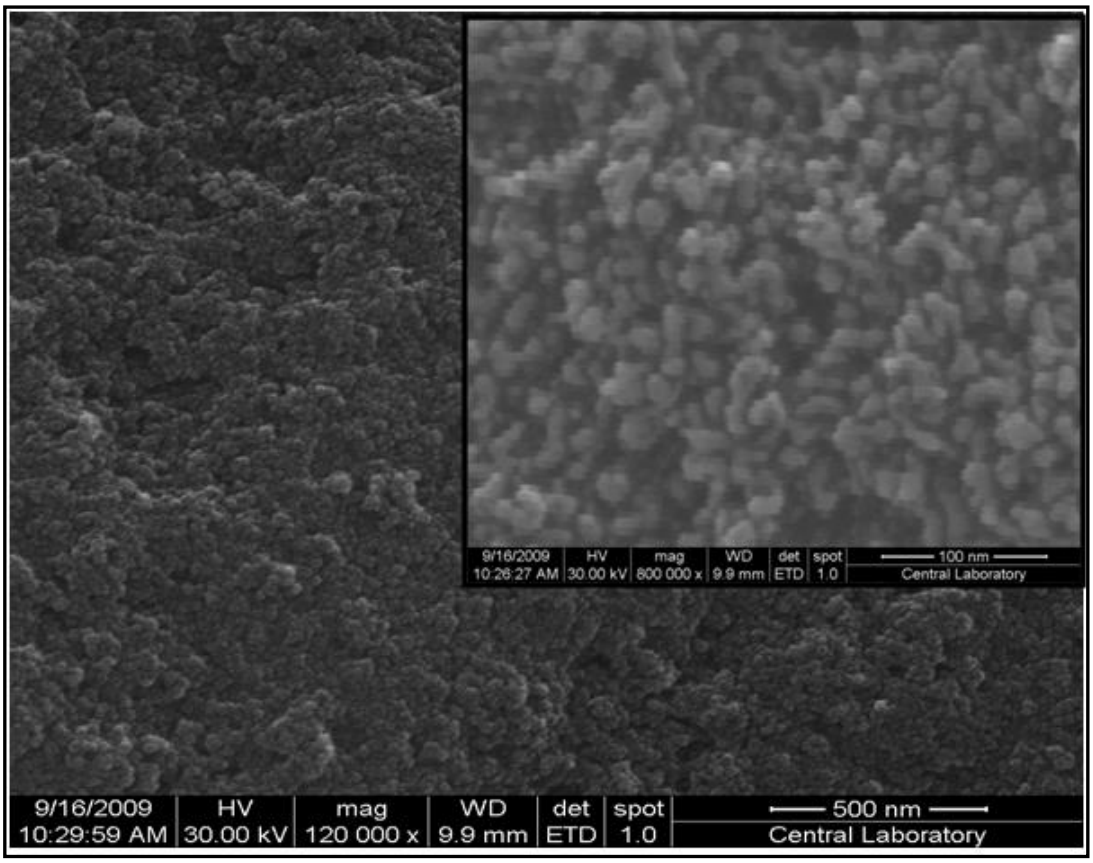

Figure 34 FE-SEM images of cobalt ferrite nanoparticles at different scales, 500 nm and 100 nm.

The number-length (arithmetic) mean size (D[1,0]) and volume weighted mean size (D[4,3]) of the primary cobalt ferrite nanoparticles counting about 100 particles from Figure 33, were calculated as, 12.9 nm and 14.06 nm, respectively (Table 6). After using NaCl as a dispersant, instead of oleic acid, the primary particle sizes were decreased.

From FE-SEM images, homogeneous size distribution of cobalt ferrite nanoparticles was clearly seen. The PDI value was 1.08 (~1.00) indicating that relativly homogeneous size distribution for the primary cobalt ferrite nanoparticles was obtained.

Table 6 The particle size results of cobalt ferrite primary nanoparticles.

Primary $CoFe_2O_4$ particles	Number-length mean size (nm) D[1,0]	Volume weighted mean size (nm) D[4,3]	Polydispersivity Index (PDI)
Dispersant: Sodium Chloride (NaCl)	12.9	14.06	1.08

The composition of the particles, determined by energy dispersive X-ray (EDX) analysis shown in Figure 35, confirmed the production of cobalt ferrite nanoparticles. EDX measurement indicated the presence of the metals employed in the preparation procedure.

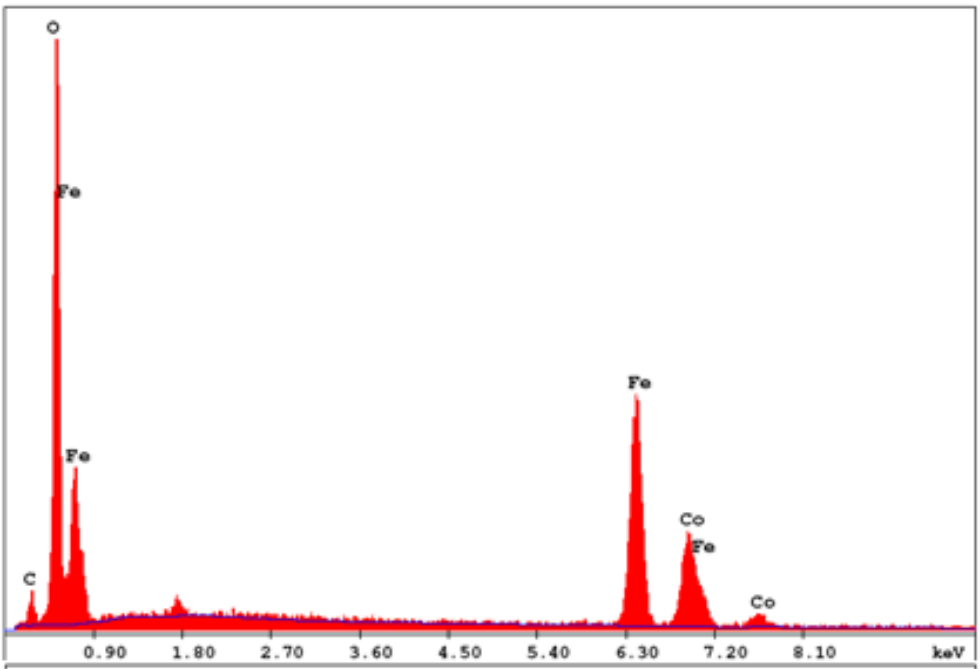

EDAX ZAF Quantification (Standardless)
Element Normalized
SEC Table : Default

Element	Wt %	At %	K-Ratio	Z	A	F
C K	7.48	15.99	0.0190	1.1014	0.2304	1.0007
O K	36.64	58.76	0.1775	1.0827	0.4468	1.0015
FeK	37.86	17.40	0.3519	0.9209	1.0092	1.0000
CoK	18.02	7.85	0.1643	0.9024	1.0102	1.0000
Total	100.00	100.00				

Element	Net Inte.	Bkgd Inte.	Inte. Error	P/B
C K	11.37	1.96	5.56	5.80
O K	278.51	2.87	0.98	96.89
FeK	209.02	4.60	1.14	45.45
CoK	82.70	3.71	1.86	22.29

Figure 35 An EDX result of cobalt ferrite nanoparticles.

The characterization of cobalt ferrite agglomerates with DLS (Zeta sizer) was given in Figure 36. The z-average mean size of the cobalt ferrite agglomerates at pH ~7 was 127.4 nm. The size distribution of the particles was in the range of 50 and 220 nm. And the PDI was given as 0.250.

The volume weighted mean size, D[4,3] (3.1.1.2.), of cobalt ferrite agglomerates was calculated as 102.7 nm. The specific surface area of cobalt ferrite agglomerates was calculated as 65.52 m^2/cm^3. The surface area of cobalt ferrite agglomerates were increased after NaCl using. NaCl increased the dispersity of cobalt ferrite agglomerates.

Table 7 The DLS (zeta sizer) results of agglomerated cobalt ferrite nanoparticles.

Agglomerated $CoFe_2O_4$ particles	Z-avarage mean size (nm)	Volume weighted mean size (nm)	Polydispersivity Index (PDI)	Specific Surface Area (m^2/cm^3)
Dispersant: NaCl	127.4	102.7	0.250	65.52

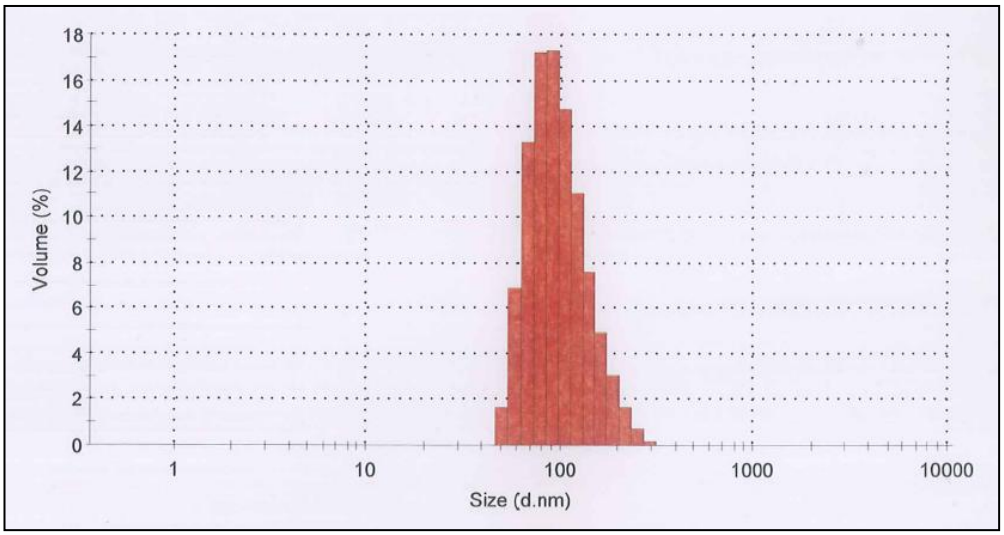

Figure 36 A histogram of cobalt ferrite agglomerates (NaCl was used as a dispersant)

The results of cobalt ferrite agglomerates have also shown that the cobalt ferrite nanoparticles have been successfully synthesized by a facile low temperature solid state reaction via the introduction of inert inorganic salt. The introduction of salt breaks up the three-dimensional network structure. As a result, the size of large agglomerates was reduced considerably and high surface area cobalt ferrite agglomerates was obtained.

3.1.3 Preparation of Cobalt Ferrite Nanoparticles in Ultrasonic Bath

In order to decrease the size of agglomerates, ultrasonic bath was used in the production of cobalt ferrite nanoparticles by using NaCl as dispersant as described in section 2.3.1.2. The image of cobalt ferrite magnetic nanoparticles obtained using ultrasonic bath was shown in Figure 37.

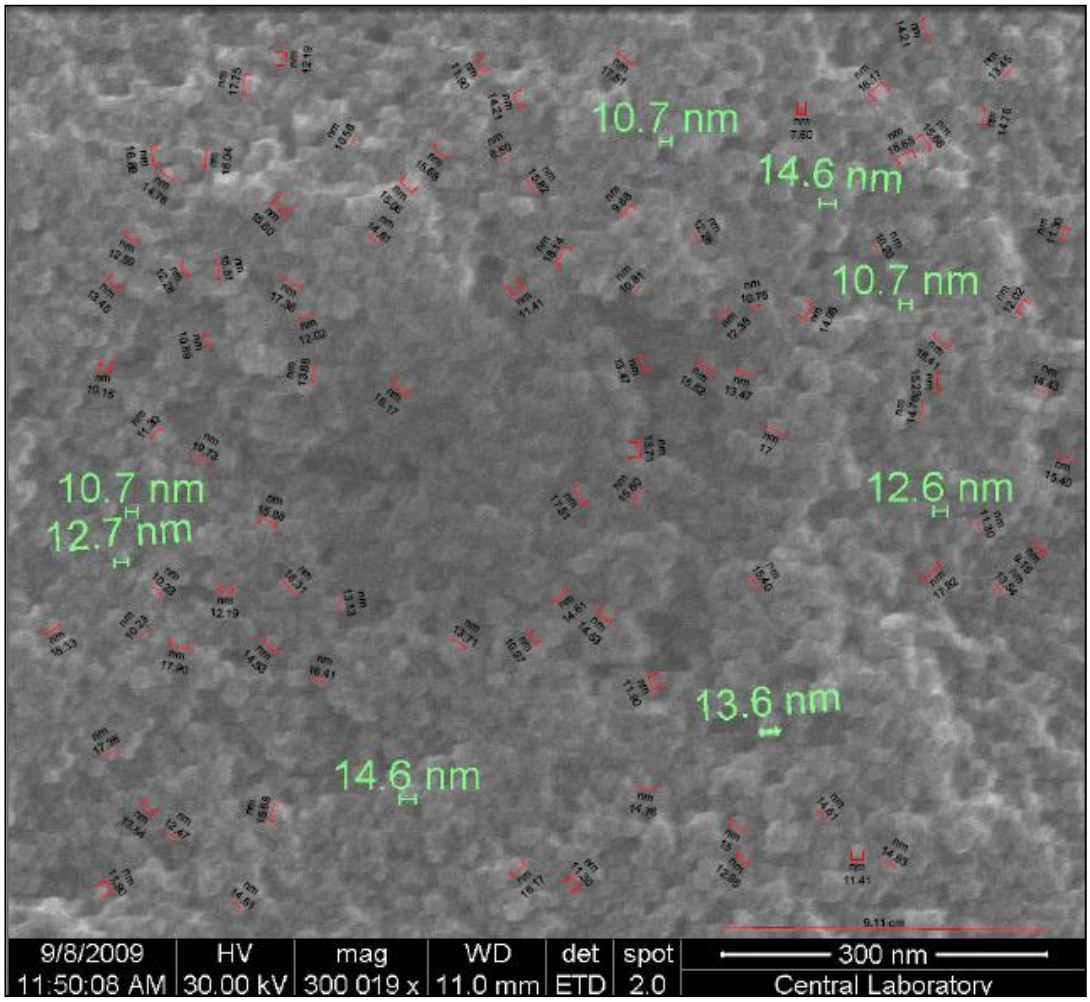

Figure 37 FE-SEM image of cobalt ferrite nanoparticles (In ultrasonic bath).

The number-length (arithmetic) mean size and volume weighted mean size of 100 primary cobalt ferrite nanoparticles were calculated as, 13.85 nm and 15.10 nm, respectively. In addition, the PDI was calculated as 1.09 (Table 8).

Table 8 The particle size results of cobalt ferrite primary nanoparticles prepared with ultrasonic bath.

Primary $CoFe_2O_4$ particles	Number-length mean size (nm) D[1,0]	Volume weighted mean size (nm) D[4,3]	Polydispersivity Index (PDI)
Dispersant: NaCl- in ultrasonic bath	13.85	15.10	1.09

From the data of Figure 38, the z-average mean size of the cobalt ferrite agglomerates was given as 128.7 nm. Size distribution of the particles was in the range of 60 and 200 nm. And the PDI of agglomerates was given as 0.151(Table 9). The specific surface area of cobalt ferrite agglomerates was calculated as 59.92 m^2/cm^3. The volume weight mean size of cobalt ferrite agglomerates was calculated as 97.3 nm.

Table 9 The DLS (zeta sizer) results of agglomerated cobalt ferrite nanoparticles prepared with ultrasonic bath.

Agglomerated $CoFe_2O_4$ particles	Z-avarage mean size (nm)	Volume weighted mean size (nm)	Polydispersivity Index (PDI)	Specific Surface Area (m^2/cm^3)
Dispersant: NaCl (ultrasonic bath)	128.7	97.3	0.151	59.92

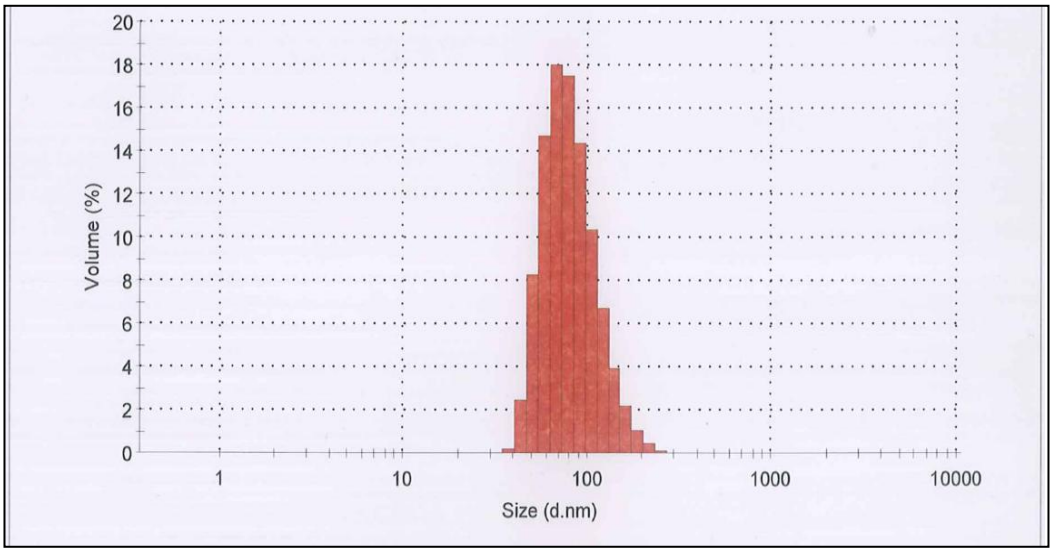

Figure 38 A histogram of cobalt ferrite nanoparticles that were synthesized in ultrasonic bath.

As a conclusion we obtained smaller size and well dispersed cobalt ferrite nanoparticles and their agglomerates by using a salt-assisted solid state method in ultrasonic bath and so this procedure was chosen and used through the study.

3.2 Silica Coating of Magnetic Cobalt Ferrite Nanoparticles

Non-toxic silica is most often used as the coating shell to provide magnetic nanoparticles soluble in water and biocompatibility in most applications. Besides, silica shell can also prevent the direct contact of the magnetic core with the environment thus avoiding undesired interactions and can be functionalized to bind molecules (Gubin, Koksharov, Khomutov, & Yu., 2005). Consequently, silica coatings have been extensively studied and many synthetic methods have been developed for various applications.

Cobalt ferrite nanoparticles were coated with silica in aqueous/ethanolic solution called as Stöber method which is described in section 2.3.2. (Kobayashi, Horie, Konno, Rodriguez-Gonzales, & Liz-Marzan, 2003). TEOS and APTMS were used for silica coating of the cobalt ferrite nanoparticles. First, APTMS solution was added into the cobalt ferrite solution and stirred for a short time. This enabled amine groups attaching on surface of the nanoparticles. Then, they were coated with silica by using TEOS with the help of amine groups provided by APTMS. Using small amount of APTMS in addition to the TEOS was very important since better silica coating was obtained compared to the procedure in which only TEOS was used. The schematic representation of the shell formation and the concentration of reagents used in the silica coating of cobalt ferrite nanoparticles was shown in Figure 39.

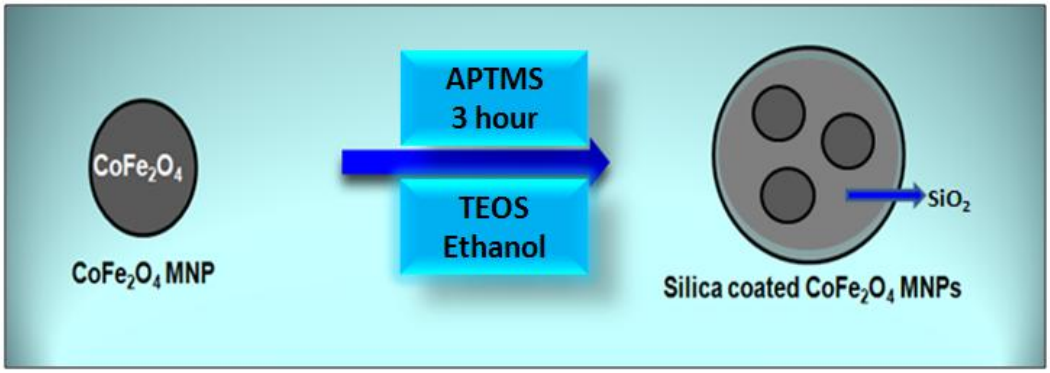

Figure 39 Synthesis of silica coated cobalt ferrite nanoparticles.

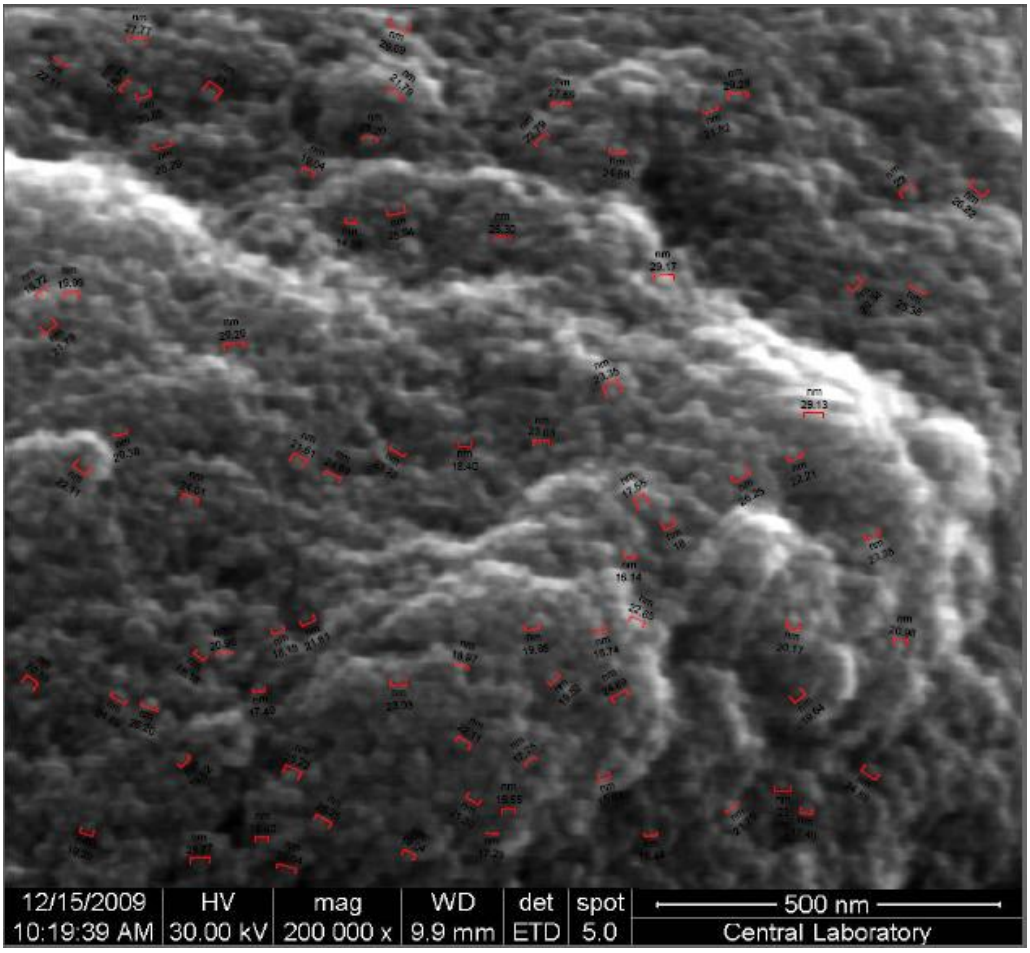

Figure 40 FE-SEM image of silica coated cobalt ferrite nanoparticles.

From Figure 40, the number-length mean size and volume weighted mean size of 100 primary silica coated cobalt ferrite nanoparticles were calculated as, 18.8 nm and 23.8 nm, respectively. In addition, the PDI was calculated as 1.27 (Table 10).

Table 10 The particle size results of silica coated cobalt ferrite primary nanoparticles.

Primary $CoFe_2O_4$ particles	Number-length mean size (nm) D[1,0]	Volume weighted mean size (nm) D[4,3]	Polydispersivity Index (PDI)
SiO_2 coated	18.8	23.8	1.27

The difference in the number-length and volume weight mean sizes of the cobalt ferrite nanoparticles and silica coated cobalt ferrite nanoparticles was attributed to the thickness of the coated silica layer. The primary particle size of uncoated cobalt ferrite nanoparticles were measured as approximately 13 nm and the silica coated ones were measured as approximately 20 nm. On average, 3.5 nm silica layer was coated on cobalt ferrite nanoparticle.

The composition of the particles, determined by energy dispersive X-ray (EDX) analysis as shown in Figure 41, confirmed cobalt ferrite core and silica shell structure for the particles. EDX measurement indicated the presence of the metals employed in the preparation procedure.

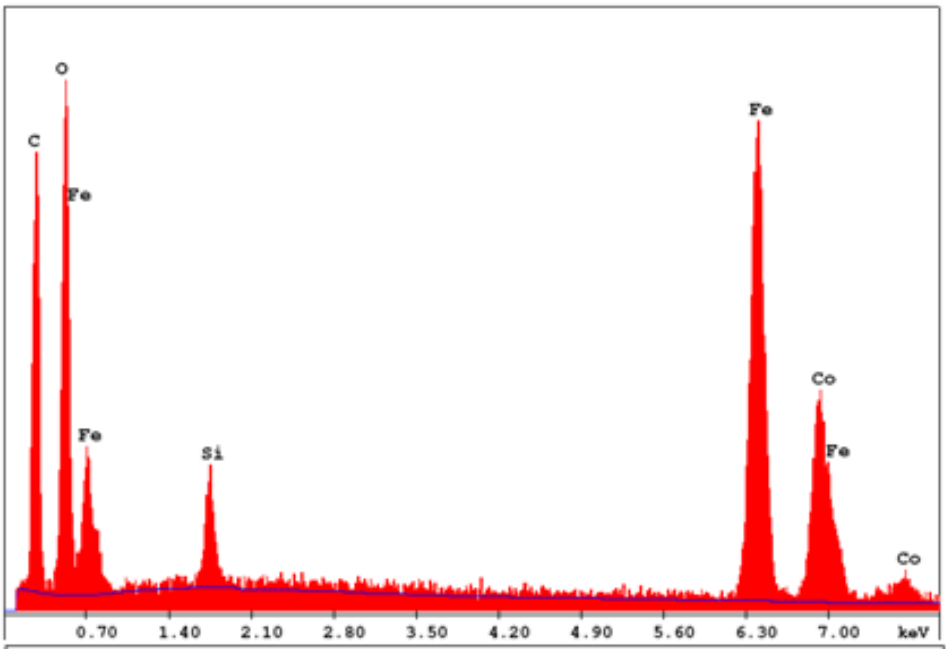

EDAX ZAF Quantification (Standardless)
Element Normalized
SEC Table : Default

Element	Wt %	At %	K-Ratio	Z	A	F
C K	43.74	58.92	0.1533	1.0337	0.3389	1.0004
O K	34.20	34.58	0.0677	1.0192	0.1941	1.0005
SiK	1.50	0.87	0.0077	0.9836	0.5217	1.0005
FeK	13.15	3.81	0.1208	0.8822	1.0400	1.0012
CoK	6.39	1.75	0.0575	0.8655	1.0390	1.0018
PbL	1.02	0.08	0.0075	0.6908	1.0688	1.0000
Total	100.00	100.00				

Figure 41 EDX results of silica coated cobalt ferrite magnetic nanoparticles.

The C signal was coming from the carbon tape used for sampling and compared to the EDX results of the uncoated cobalt ferrite nanoparticles (Figure 41). The presence of silicon peak on the spectrum was considered as the indication of silica layer formation on the surface of cobalt ferrite nanoparticles.

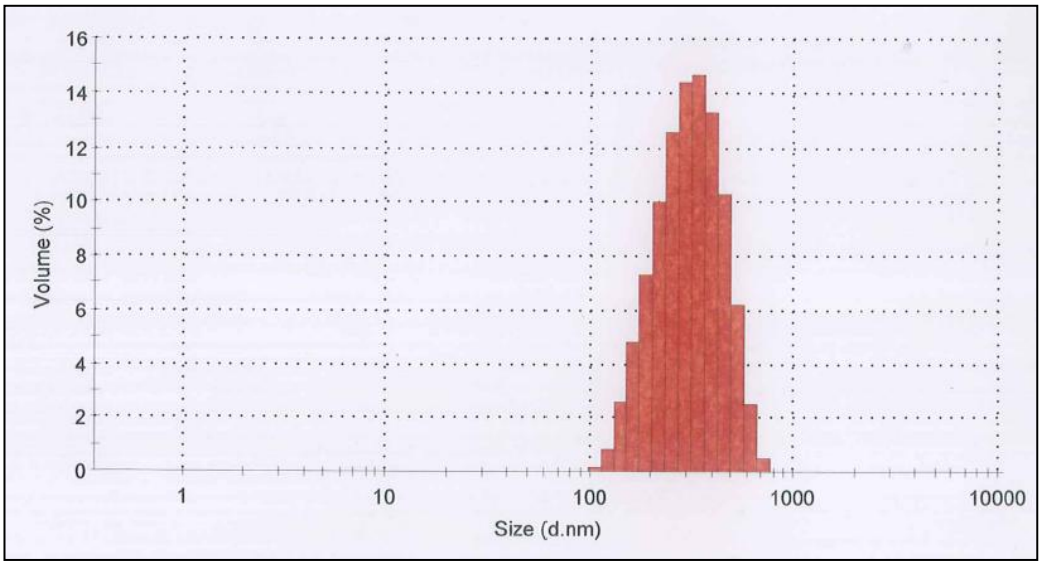

Figure 42 A histogram of silica coated cobalt ferrite nanoparticles.

Size distribution of the particles was observed in the range of 141 and 712 nm from the histogram (Figure 42). The z-average mean size of silica coated $CoFe_2O_4$ agglomerates at pH ~7 was 267.0 nm. And the PDI of them was given as 0.111 (Table 11). The volume weighted mean size of silica coated cobalt ferrite agglomerates was calculated as 325.3 nm. And the specific surface area of cobalt ferrite agglomerates was calculated as 21.13 m^2/cm^3.

Table 11 The DLS (zeta sizer) results of silica coated- agglomerated cobalt ferrite nanoparticles.

Agglomerated $CoFe_2O_4$ particles	Z-avarage mean size (nm)	Volume weighted mean size (nm)	Polydispersivity Index (PDI)	Specific Surface Area (m^2/cm^3)
SiO_2 coated	267.0	325.3	0.111	21.13

FT-IR analysis was done in order to investigate the bonds concerning the silica layer formed on cobalt ferrite nanoparticles. FT-IR spectra of these nanoparticles was shown in Figure 43.

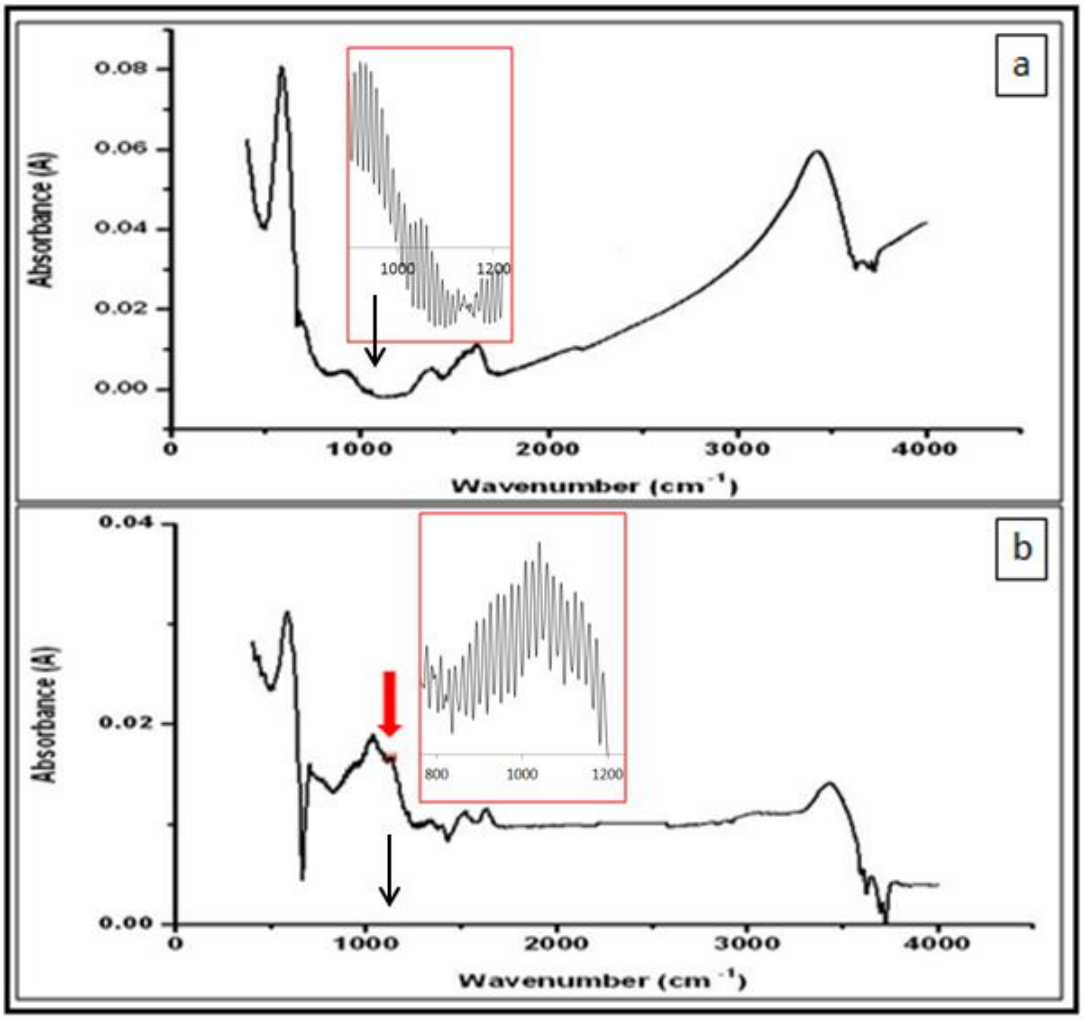

Figure 43 FT-IR results of (a) cobalt ferrite nanoparticles and (b) silica coated cobalt ferrite nanoparticles.

As can be seen from Figure 43-b, asymmetric stretching of Si-O-Si vibrations was observed at 1080 cm^{-1}. Its appearance was correlated with the coating of silica layer on cobalt ferrite nanoparticles.

3.3 Magnetic Behavior of the Prepared Particles

3.3.1 Magnetic Behavior of Cobalt Ferrite Nanoparticles

Magnetic behavior of the particles prepared with ultrasonic bath was simply investigated by their collection under the influence of external magnetic field for each batch. Results are shown in Figure 44.

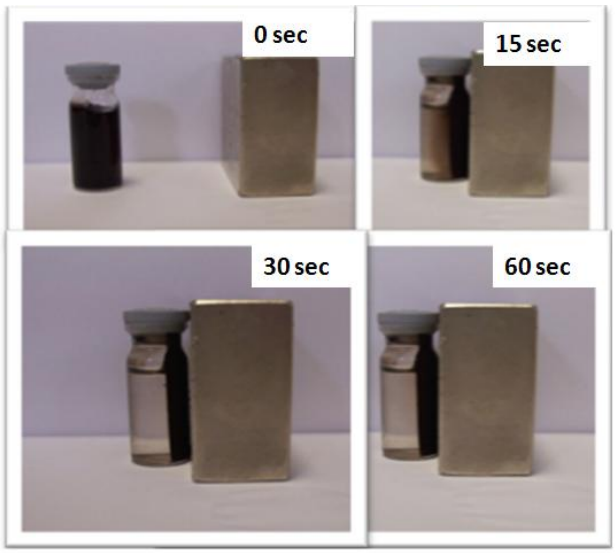

Figure 44 Magnetic behavior of cobalt ferrite nanoparticles after external magnetic field was applied (1.6T).

As can be seen from the Figure 44, particle collection was complete after 60 seconds. The magnetic property of the cobalt ferrite nanoparticle was characterized by vibrating sample magnetometer (VSM). Hysteresis curve of cobalt ferrite recorded at 300K was illustrated in Figure 45.

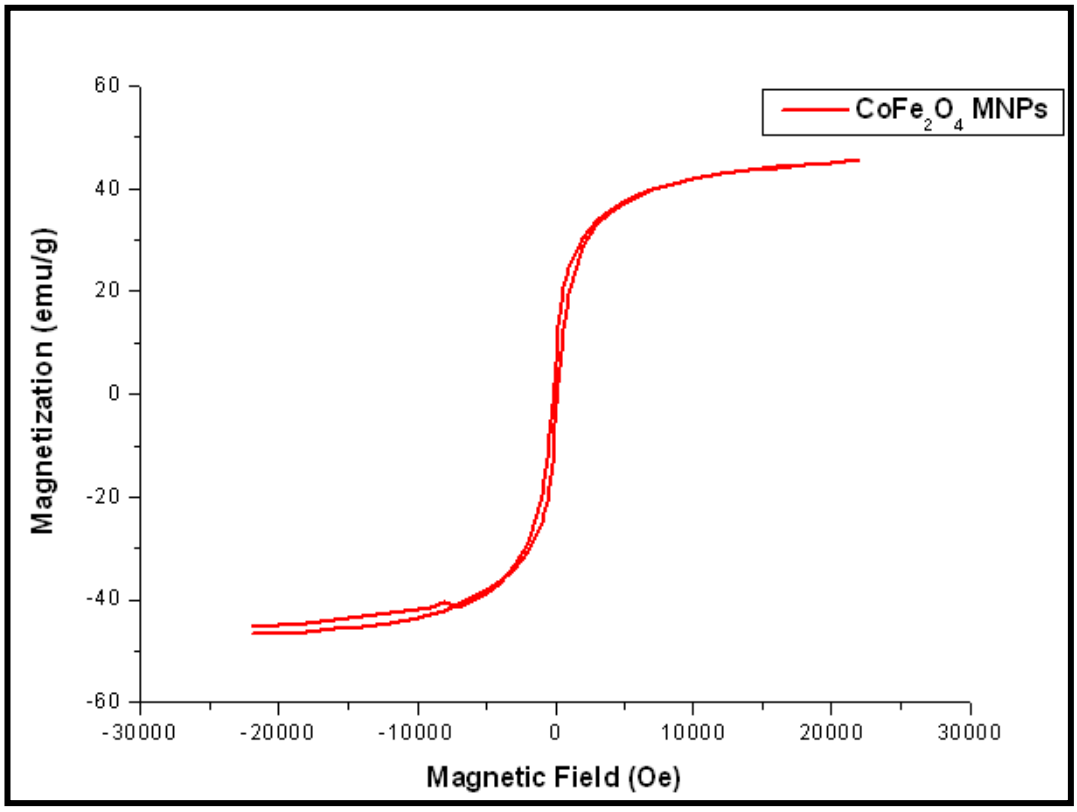

Figure 45 Hysteresis curve of cobalt ferrite nanoparticles recorded at 300K and at a maximum magnetic field of 2.2 Tesla

Saturation magnetization and the coerctivity values of cobalt ferrite magnetic nanoparticles were measured as 46.16 emu/g and was 147.0 Oe, respectively.

3.3.2 Magnetic Behavior of Silica Coated Cobalt Ferrite Nanoparticles

To examine the change in the magnetization of cobalt ferrite nanoparticles after silica coating, a simple collection rate experiment under magnetic field was applied. Silica coated cobalt ferrite nanoparticles were collected magnetically when external magnet is next to the solution as depicted in the Figure 46. The collection was as rapid as in the case of cobalt ferrite nanoparticles; it takes approximately 60 seconds to obtain clear solution.

Figure 46 Magnetic behavior of silica coated cobalt ferrite nanoparticles, after external magnetic field (1.6T) applied. Particles were collected in 60 seconds.

Magnetic property of silica coated cobalt ferrite nanoparticles were also characterized by vibrating sample magnetometer. Hysteresis curve of silica coated cobalt ferrite was recorded at 300K illustrated in Figure 47.

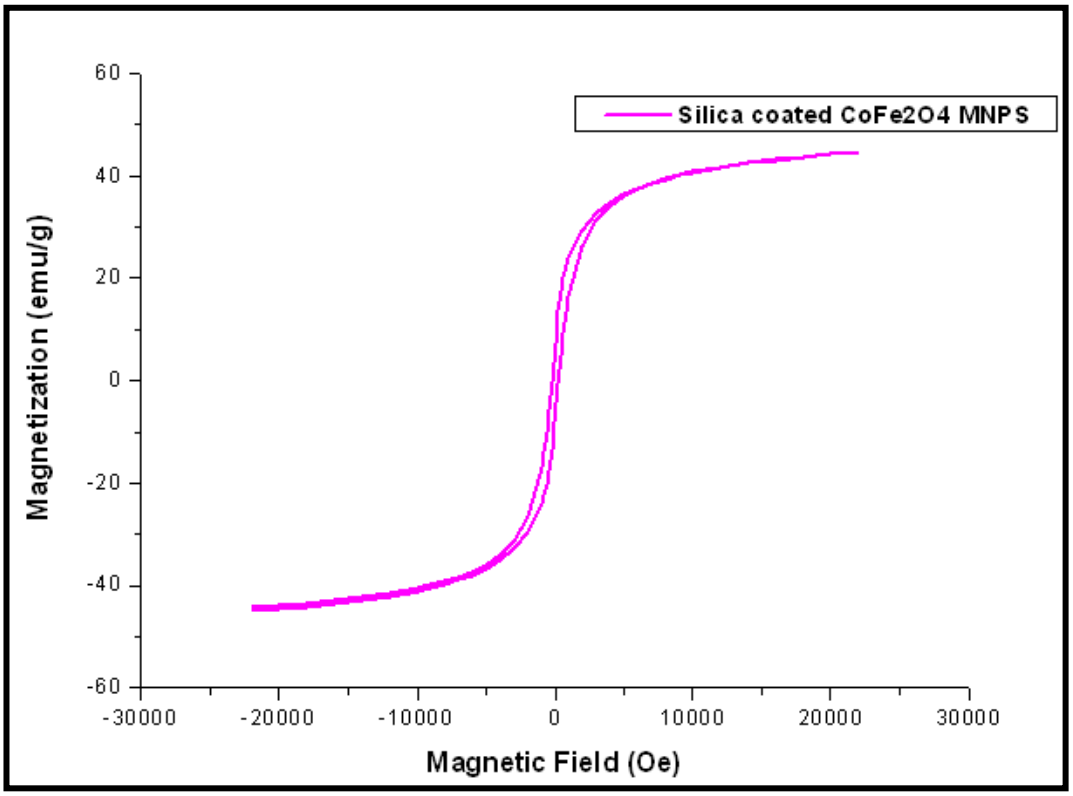

Figure 47 Hysteresis curve of silica coated cobalt ferrite nanoparticles recorded at 300K and at a maximum magnetic field of 2.2 Tesla.

Saturation magnetization value of silica coated cobalt ferrite magnetic nanoparticles was 44.7 emu/g and the coactivity value was 202.5 Oe. Compared to cobalt ferrite nanoparticles, magnetization value (emu/g) decreased slightly due to the presence of nonmagnetic silica coating.

3.4 Addition of Amine and Carboxyl Functional Groups on Silica Coated Cobalt Ferrite Nanoparticles

Amine functionalization was carried out according to the Stöber reaction as given in the experimental section 2.3.2. . After addition of amine group on silica coating of cobalt ferrite nanoparticle, carboxyl groups were added by using ring opening linker elongation reaction (An, Chen, Xue, & Liu, 2007). In this process glutaric anhydride ring structure was opened and reacted with the amine groups. The schematic representation of the surface modification of silica coated cobalt ferrite nanoparticles was shown in Figure 48.

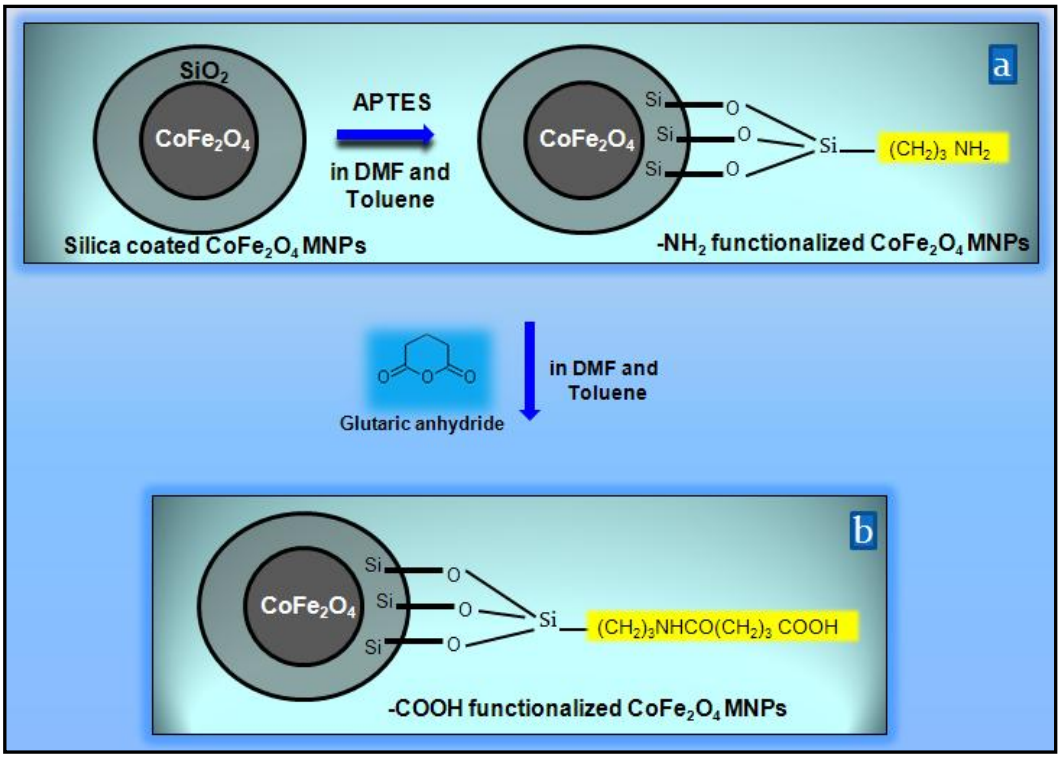

Figure 48 Functionalization of silica coated cobalt ferrite nanoparticles with (a) –NH_2 and (b) –COOH functional groups.

FT-IR spectrometer was used for the characterization of the amine and carboxyl groups introduced on the surface of silica coated cobalt ferrite nanoparticles. FT-IR spectra of the amine and carboxyl modified silica coated magnetite nanoparticles are shown in Figure 49.

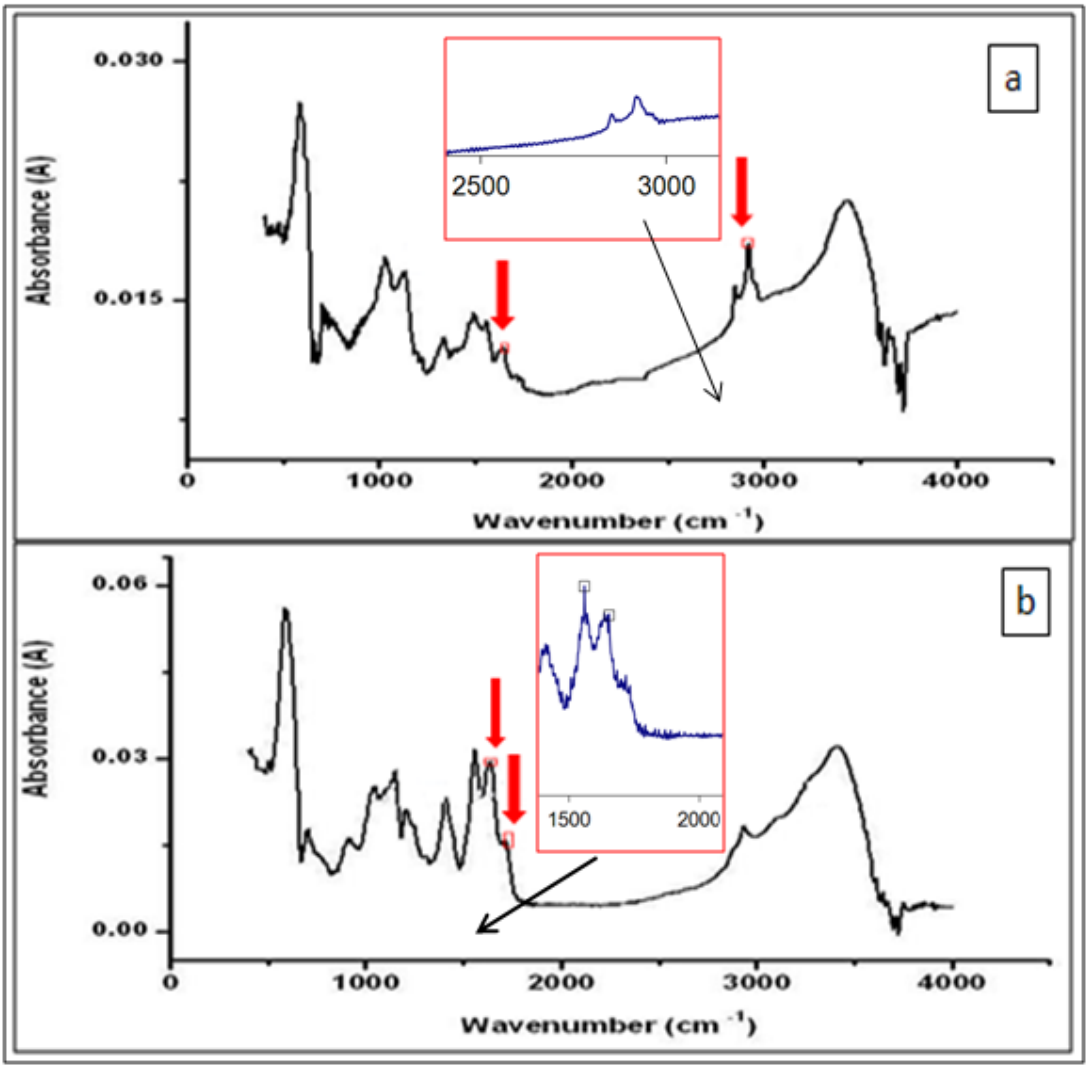

Figure 49 FTIR results of (a) $–NH_2$ modified and (b) –COOH functionalized cobalt ferrite nanoparticles.

FTIR spectra of the silica coated cobalt ferrite nanoparticles functionalized by $–NH_2$ groups and by -COOH groups are shown in Figure 49. The characteristic absorption peaks of –COOH at 1718.6 cm^{-1} and –NHCO– at 1556.4 cm^{-1} are observed in the spectrum of the –COOH group functionalized silica-coated cobalt ferrite nanoparticles. Combined with the band in the range 2920–2980 cm^{-1}, corresponding to the $–CH_2$ stretching vibration in (a) and (b), one can deduce that –
NH_2 groups are bonded to the surface through a reaction of –OH and APTES. This is a strong evidence that –COOH groups were bonded to the surface through a reaction of $–NH_2$ and glutaric anhydride, as indicated in Figure 48. The absorption bands at about 3427.8 and 1637.6 cm^{-1} in all the spectra mainly originate from the OH vibrations in H_2O (He, Wang, Li, Miao, Wu, & Zou, 2005).

3.5 NTA Modified Magnetic Cobalt Ferrite Nanoparticles

Surface modification of the silica coated cobalt ferrite nanoparticles by amine and carboxyl groups was followed by the addition of NTA (Nα,Nα-Bis(carboxymethyl)-L-lysine hydrate) groups onto the nanoparticles. The structure of NTA was shown at Figure 50. It has carboxyl and amine ends. NTA was covalently bound to the carboxylic acid end group of −COOH modified cobalt ferrite nanoparticle structure (Figure 51).

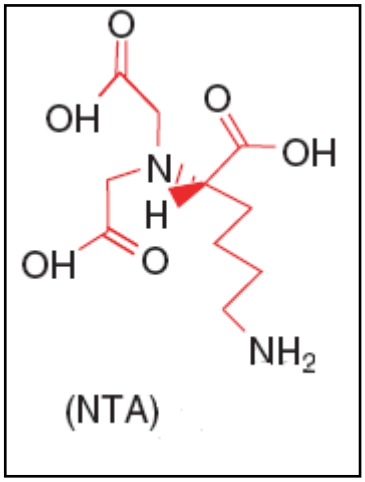

Figure 50 The structure of NTA (Nα,Nα-Bis(carboxymethyl)-L-lysine hydrate).

NTA molecules were attached to the –COOH groups on the surface as shown in Figure 51.

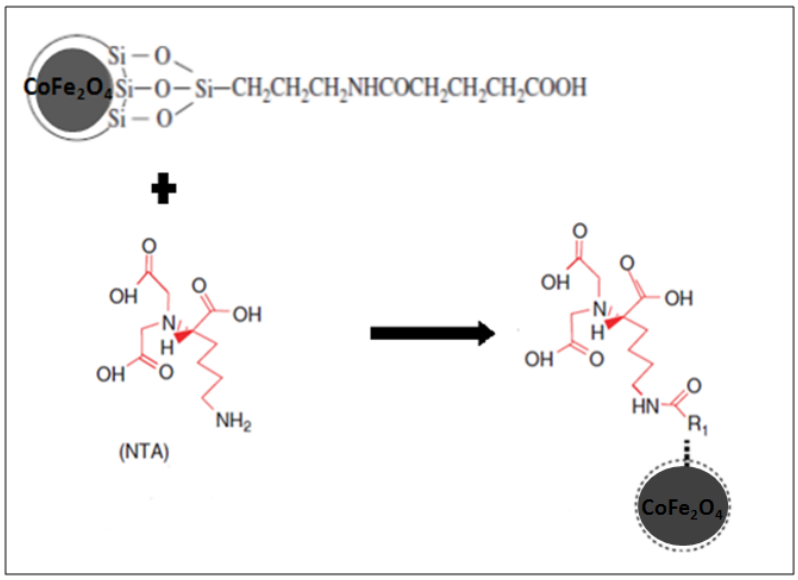

Figure 51 Attachment of a NTA molecule to the –COOH free group on the surface of cobalt ferrite nanoparticle.

NTA modified nanoparticles were characterized by FTIR. The FTIR spectra of pure NTA (a) and NTA modified cobalt ferrites (b) were shown in Figure 52.

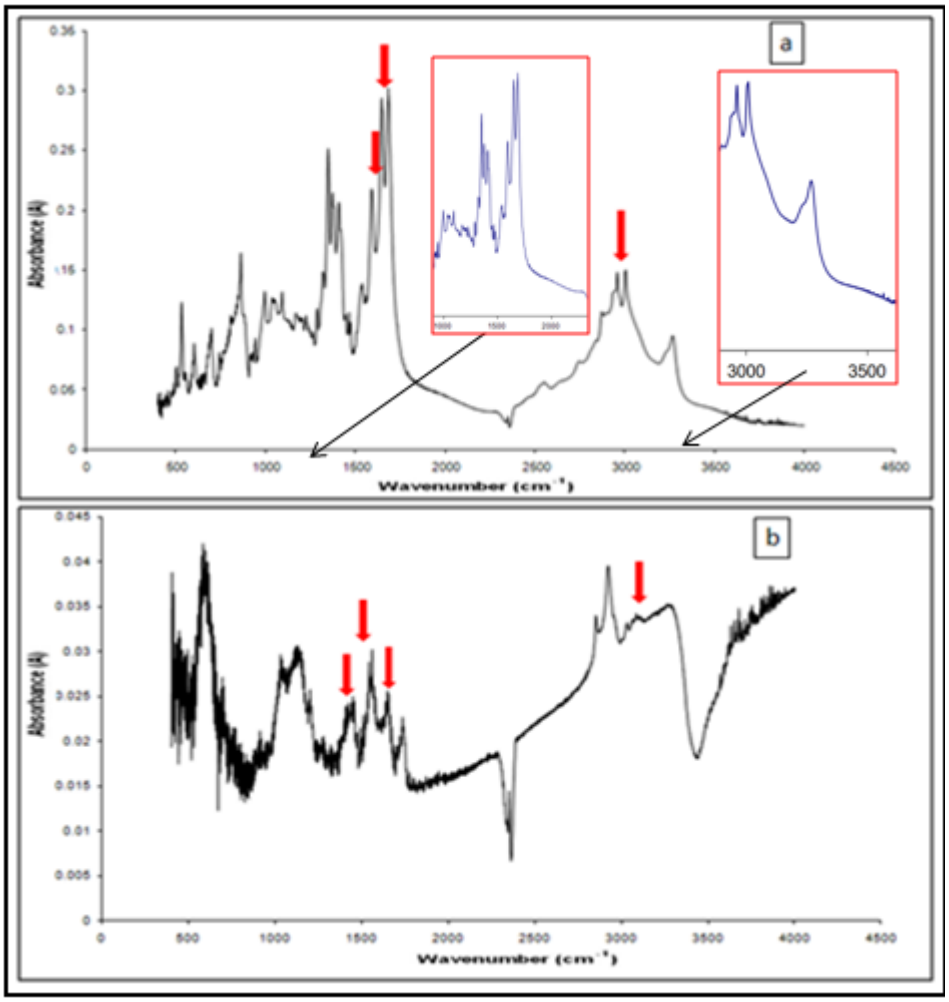

Figure 52 (a) FT-IR results of pure NTA and (b) NTA modified cobalt ferrite nanoparticles.

The peaks that were observed between the ranges 3500-3200 cm^{-1} were related to $-NH_2$ stretching vibrations of the NTA. Symmetric stretching vibration peaks of the deprotonated carboxylic groups were located at 1380 cm^{-1}.The asymmetric vibration of the deprotonated carboxylic group peak was observed at ~1615 cm^{-1} (Tural, Kaya, Özkan, & Volkan, 2008).

3.6 Attachment of Ni (II) Ions to NTA Modified Cobalt Ferrite Nanoparticles

The quadridentate NTA moiety covalently coupled to the surface of silica coated cobalt ferrite nanoparticles via spacer butyl amine arm. The remaining four chelating sites of the modified NTA interact with nickel (II), which results binding of ions (Figure 53).

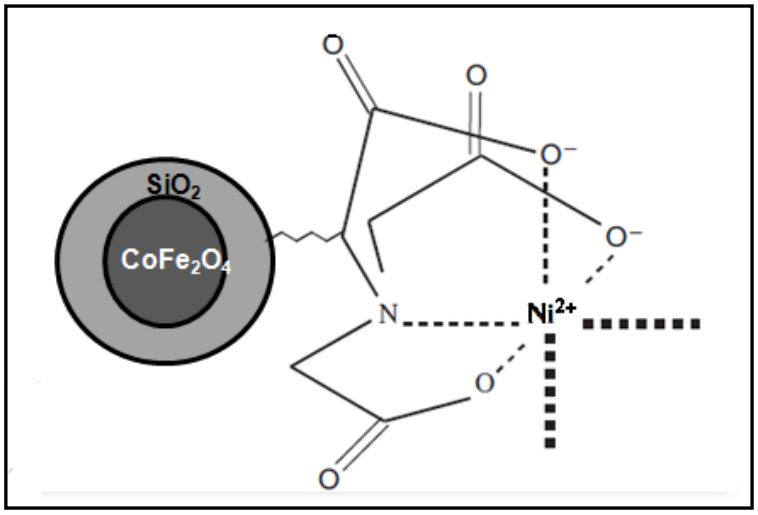

Figure 53 Structure of the NTA modified cobalt ferrite nanoparticles after Ni (II) ion attachment (Tural, Kaya, Özkan, & Volkan, 2008).

The silica coated cobalt ferrite nanoparticles functionalized with NTA were loaded with Ni (II) ions. Quantification of Ni (II) binding was done using inductively coupled plasma spectrometry (ICP-OES). The concentration of the Ni (II) ions in the loading solution prior to the addition of the magnetic nanoparticles and in the supernatant solution after removing the magnetic nanoparticles were measured by ICP-OES. 12.9 mg NTA modified cobalt ferrite nanoparticles were put in to 25 ml, 20 mg/l Ni (II) ion solution for loading. After mixing, nanoparticles were collected by applying external magnetic field.

The supernatant solution was kept for ICP-OES measurements to determine the amount of Ni (II) ions. The calibration line of the nickel standards and the calibration equation were shown in Figure 54.

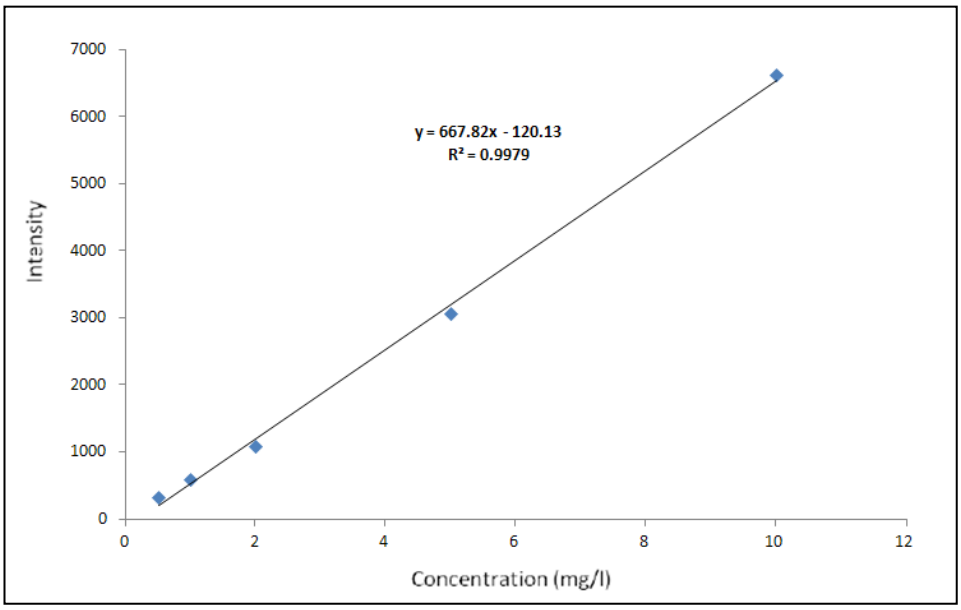

Figure 54 Calibration curve of nickel standard solution.

By using calibration line shown in the upper figure, the amount of Ni (II) ions attached to NTA coated cobalt ferrite nanoparticles was calculated. As a result, 6.15 mg/L Ni (II) ions were bonded to 0.0148 g surface modified cobalt ferrite nanoparticles. This result also revealed the existence of NTA on the surface of silica coated cobalt ferrite nanoparticles. After immobilization of the Ni-NTA affinity group, the remaining two free sites of ions are ready to bind histidine-tagged proteins through the use of imidazole side chains of histidine molecules. Silica coated-cobalt ferrite nanoparticles retained their magnetic properties, suggesting that they can be used in the magnetic separation of histidine-tagged proteins.

CHAPTER 4

CONCLUSION

In this study, cobalt ferrite magnetic nanoparticles were synthesized by co-precipitation methods. According to this procedure Fe (III) and Co (II) salts were precipitated by adding a base. In order to get small size of agglomerates, different type of dispersants (oleic acid, sodium chloride) and washing solutions (ethanol, deionized water, and acetone) were tried. After obtaining appropriate dispersant, ultrasound was applied to further decrease the size of nanoparticle agglomerates. FE-SEM was used to observe the morphology and the size distribution of the $CoFe_2O_4$ nanoparticles and the size of the agglomerates were measured by using dynamic light scattering (zeta-sizer) to show particle size distribution trend. From FE-SEM images, the number-length mean size and the volume weighted mean size of primary cobalt ferrite particles which were prepared with oleic acid, were calculated as 25.1 nm and 27.4 nm, respectively. The z-average mean size of the $CoFe_2O_4$ agglomerates at pH ~7 was 147.4 nm. In the case of sodium chloride as dispersant, the number-length mean size and the volume weighted mean size of primary cobalt ferrite nanoparticles, were calculated as 12.9 nm and 14.1 nm, respectively. The z-average mean size of the $CoFe_2O_4$ agglomerates at pH ~7 was 127.4 nm. The primary particle sizes and z-average mean size of the agglomerates were decreased by applying sodium chloride in the preparation procedure. According to these results, NaCl was used as a dispersant and applied through the study. By applying ultrasound the number-length mean size and the volume weighted mean size of primary cobalt ferrite nanoparticles, were calculated as 13.85 nm and 15.10 nm, respectively and the z-average mean size of the agglomerates was given as 128.7 nm. Saturation magnetization value of cobalt

ferrite magnetic nanoparticle thus prepared was measured as 46.16 emu/g by using VSM.

The surface of cobalt ferrite nanoparticles were coated with silica shell by using hydrolyze/condensation reactions of tetraethyl orthosilicate (TEOS) and 3-aminopropyl-trimethoxysilane (APTMS). Silica coated cobalt ferrite nanoparticles were characterized by FE-SEM, DLS (zeta sizer), FT-IR and VSM. The number-length mean size and the volume weighted mean size of primary silica coated cobalt ferrite nanoparticles were calculated as 18.8 nm and 23.8 nm. The primary particle size of uncoated was measured as approximately 13 nm and the silica coated ones were measured as approximately 20 nm. On average, 3.5 nm silica layer was coated on cobalt ferrite nanoparticle. Magnetic properties were characterized by VSM. Saturation magnetization value of silica coated cobalt ferrite magnetic nanoparticles was evaluated as 44.7 emu/g. Due to the introduction of nonmagnetic silica layer onto the magnetic particles, the saturation magnetization value was decreased about 1.46 emu/g compared to the uncoated ones. Further functionalization of nanoparticles were done by adding carboxyl (-COOH) functional groups on to surface of silica coated cobalt ferrite nanoparticles. After that Nα,Nα-Bis(carboxymethyl)-L-lysine hydrate (NTA) added to the end of the carboxyl groups of modified cobalt ferrite structure. The functional groups were characterized by FTIR. Finally Ni (II) ions were attached to NTA. Ni (II) ion concentration was determined by ICP-OES. As a result, 6.15 mg/L Ni (II) ions were bonded to 0.0148 g surface modified cobalt ferrite nanoparticles. For further studies, these prepared Ni (II) ion loaded cobalt ferrite nanoparticles will be used in protein separation and purification and catalysis applications.

REFERENCES

An, Y., Chen, M., Xue, Q., & Liu, W. (2007). Preparation and self-assembly of carboxylic acid-functionalized silica. J. Colloid Interface Sci. 311 , 507-513.

Berensmeier, S. (2006). Magnetic particles for the separation and purification of nucleic acids. Appl. Microbiol. Biotechnol. , 73, 495-504.

Berry, C., & Curtis, A. (2003). Functionalization of magnetic nanoparticles for application in biomedicine. J. Phys. D: Appl. Phys. , 36, R198.

Bucak, S., Jones, D., Laibinis, P., & Hatton, T. (2003). Biotechnol. Progr. , 19, 477.

Callister, W. (2007). Materials science and engineering: An Introduction. New York: Jonn Wiley & Sons .

Chinnasamy, C., Senoue, M., Jeyadevan, B., Perales-Perez, O., Shinoda, K., & Tohji, K. (2003). Synthesis of size-controlled cobalt ferrite particles with high coercivity and squareness ratio. J. Colloid Interface Sci. , 263, 80.

De, M., Chosh, P., & Rotello, V. (2008). Applications of nanoparticles in biology. Adv. Mater. , 20, 1.

Fu, L., Dravid, V., Klug, K., Liu, X., & Mirkin, C. (2002). Synthesis and patterning of magnetic nanostructures. Eur. J. Cell Biol. and Mater. , 156.

Goldman, A. (1990). Modern Ferrite Technology. New York : Springer.

Gu, H., Ho, P., Tsang, K., Wang, L., & Xu, B. (2003). Synthesis and characterization of functionalized silica-coated Fe_3O_4 superparamagnetic nanocrystals for biological applications. J. Am. Chem. Soc. , 125, 15702.

Gubin, S., Koksharov, Y. A., Khomutov, G., & Yu., Y. G. (2005). Magnetic nanoparticles: preparation, structure and properties. Russ. Chem. Rev. , 74(6), 489-520.

Gyergyek, S., Makovec, D., Kodre, A., Arcon, I., Jagodic, M., & Drofenik, M. (2009). Influence of synthesis method on structural and magnetic properties of cobalt ferrite nanoparticles. J. Nanopart. Res. ,12, 1263-1273.

He, Y., Wang, S., Li, C., Miao, Y., Wu, Z., & Zou, B. (2005). Synthesis and Characterization of functionalized silica coated Fe_3O_4 superparamagnetic nanocrystals for biological applications. J. Phys. D: Appl. Phys. 38 , 1342-1350.

Jia, X., Chen, D., Jiao, X., He, T., Wang, H., & Jiang, W. (2008). Monodispersed Co, Ni-ferrite nanoparticles with tunable sizes: controlled synthesis, magnetic properties, and surface modification. J. Phys. Chem.C , 112, 911-917.

Jun, Y.-W., Seo, J.-W., & Cheon, J. (2008). Nanoscaling laws of magnetic nanoparticles and their applicabilities in biomedical sciences. Acc. Chem. Res. , 41 (2), 179-189.

Kobayashi, Y., Horie, M., Konno, M., Rodriguez-Gonzales, B., & Liz-Marzan, L. (2003). Preparation and properties of silica coated cobalt nanoparticles. J. Phys. Chem. B, 107 , 7420-7425.

Lee, I., Lee, N., Park, J., Kim, B., Yi, Y.-W., Kim, T., et al. (2006). Ni/NiO core/shell nanoparticles for selective binding and magnetic separation of histidine-tagged proteins. J. Am. Chem. Soc. , 10658-10659.

Li, X.-H., Xu, C. L., Han, X.-H., Qiao, L., Wang, T., & Li, F. (2010). Synthesis and magnetic properties of nearly monodisperse $CoFe_2O_4$ nanoparticles through a simple hydrothermal condition. Nanoscale Res. Lett. , 5, 1039-1044.

Liang, Y., Zhang, L., & Jian, W. (2007). Magnetic particle-based hybrid platforms for bioanalytical sensors. Chem. Phys. Chem. , 8, 2367.

Lu, A.-H., Salabas, E., & Schüth, F. (2007). Magnetic nanoparticles: synthesis , protection, functionalization, and application. Angew. Chem. Int. Ed. 46 , 1222-1244.

Maaz, K., Mumtaz, A., Hasanain, S., & Ceylan, A. (2007). Synthesis and magnetic properties of cobalt ferrite nanoparticles prepared by wet chemical route. Journ. Magn. Magn. Mater. 308 , 289-295.

Nagarajan, R., & Hatton, T. (2008). Nanoparticles: Synthesis, Stabilization, Passivation and Functionalization. Washington, DC: ACS.

Pankhurst, Q., Connolly, J., Jones, S., & Dobson, J. (2003). Applications of magnetic nanoparticles in biomedicine. J. Phys. D: Appl. Phys. 36 , R167-R181.

Parton, E., De Palma, R., & Borghs, G. (2007, August). Biomedical applications using magnetic nanoparticles. Solid State Technol. , 48.

Patel, G. (2007). Nanomedical Devices: An Owerviev. G. Patel, Nanomedical Devices: An Owerviev (5). Pharmainfo.net.

Peacock, R. (1966). The Chemistry of Technetium and Rhenium. Amsterdam, London, New York: Elsevier Publishing Company.

Pillai, V., & Shah, D. (1996). Synthesis of high-coercivity cobalt ferrite particles using water-in-oil microemulsions. J. Magn. Magn. Mater. , 163, 243.

Qin, R., Li, F., Jiang, W., & Liu, L. (2009). Salt-assisted low temperature solid state synthesis of high surface area $CoFe_2O_4$ nanoparticles. J. Mater. Sci. Technol. 25, 1 , 69-72.

Ralls, K., Courtney, T., & Wulff, J. (1976). Introduction to Materials Science and Engineering. New York: Jhon Wiley& Sons.

Rawle, A. (2002). The importance of particle sizing to the coatings industry; Part 1: Particle size measurement. Advances in Colour Science and Technology , 1-12.

Safarik, I., & Safarikova, M. (2002). Magnetic nanoparticles and biosciences. Chem. Mon. , 133, 737.

Shylesh, S., Schünemann, V., & Thiel, W. (2010). Magnetically separable nanocatalysts: bridges between homogeneous and heterogeneous catalysis. Angew. Chem. Int. Ed. , 49, 3428-3459.

Spaldin, N. A. (2003). Magnetic Materials; Fundamentals and Applications. New York: Cambridge, University Press.

Sun, S., & Zeng, H. (2002). Size-controlled synthesis of magnetite nanoparticles. J. Appl. Chem. Soc. , 124, 8204.

Sun, S., Zeng, H., Robinson, D., Raoux, S., Rice, P., Wang, S., et al. (2004). Monodisperse MFe_2O_4 (M = Fe, Co, Mn) Nanoparticles. J. Appl. Chem. Soc. , 126, 273.

Tabriz, M. F., Salehpour, P., & Kandjani, A. E. (2011). Application of artificial neural networks in optical properties of nanosemiconductors. M. F. Tabriz, P. Salehpour, & A. E. Kandjani , Artificial Neural Networks- Application (s. 479-496). Croatia: InTech.

Tartaj, P., Morales, M. P., Veintemillas-Verdaguer, S., Gonzalez-Carreno, T., & Serna, C. (2003). The preparation of magnetic nanoparticles for applications in biomedicine. J.Phys.D: Appl. Phys. 36 , R182-R197.

Toksha, B., Shirsath, S., Patange, S., & Jadhav, K. (2008). Structural investigations and magnetic properties of cobalt ferrite nanoparticles prepared by sol-gel auto combustion methods. Solid State Commun. 147 , 479-483.

Tural, B., Kaya, M., Özkan, N., & Volkan, M. (2008). Preparation and characterization of Ni-Nitriloacetic acid bearing poly(methacrylic acid) coated superparamagnetic magnetite nanoparticles. J. Nanosci. Nanotechnol. , 8, 695-701.

Vo-Dihn, T. (2005). Protein Nanotechnology: Protocols,Instrumentation, and Applications. New Jersey: Humana Press.

Voutou, B., & Stefanaki, E.-C. (2008). Electron Microscopy: The Basis. Phys. Adv. Mater. , 2-11.

Willard, M., Kurihara, L., Carpenter, E., Calvin, S., & Harris, V. (2004). Chemically prepared magnetic nanoparticles. Int. Mate.Rew. , 49 (3-4), 125-170.

Wu, M., Zhang, Y., Hui, S., Xiao, T., Ge, S., Hines, W., et al. (2002). Magnetic properties of SiO_2-coated Fe nanoparticles. J. Appl. Phys. , 92 (11), 6809-6812.

Xu, C., Xu, K., Gu, H., Zhong, X., Guo, Z., Zheng, R., et al. (2004). Nitrilotriacetic acid-modified magnetic nanoparticles as a general agent to bind histidine-tagged proteins. J. Am. Chem. Soc. , 126 (11), 3392-3393.